

B-cell antigen receptor expression and phosphatidylinositol 3-kinase signaling regulate genesis and maintenance of mouse chronic lymphocytic leukemia

Vera Kristin Schmid,¹ Ahmad Khadour,¹ Nabil Ahmed,² Carolin Brandl,³ Lars Nitschke,³ Klaus Rajewsky,⁴ Hassan Jumaa¹ and Elias Hobeika¹

¹Institute of Immunology, University Medical Center Ulm, Ulm; ²Uniklinik RWTH Aachen, Aachen; ³Division of Genetics, Department of Biology, Friedrich Alexander University Erlangen-Nürnberg, Erlangen and ⁴Max Delbrück Center for Molecular Medicine, Berlin, Germany

Correspondence:

Elias Hobeika
elias.hobeika@uni-ulm.de

Received: September 1, 2021.

Accepted: January 4, 2022.

Prepublished: January 13, 2022.

<https://doi.org/10.3324/haematol.2021.279924>

©2022 Ferrata Storti Foundation

Haematologica material is published under a CC-BY-NC license 

Abstract

Chronic lymphocytic leukemia (CLL) is a frequent lymphoproliferative disorder of B cells. Although inhibitors targeting signal proteins involved in B-cell antigen receptor (BCR) signaling constitute an important part of the current therapeutic protocols for CLL patients, the exact role of BCR signaling, as compared to genetic aberration, in the development and progression of CLL is controversial. In order to investigate whether BCR expression *per se* is pivotal for the development and maintenance of CLL B cells, we used the TCL1 mouse model. By ablating the BCR in CLL cells from TCL1 transgenic mice, we show that CLL cells cannot survive without BCR signaling and are lost within 8 weeks in diseased mice. Furthermore, we tested whether mutations augmenting B-cell signaling influence the course of CLL development and its severity. The phosphatidylinositol-3-kinase (PI3K) signaling pathway is an integral part of the BCR signaling machinery and its activity is indispensable for B-cell survival. It is negatively regulated by the lipid phosphatase PTEN, whose loss mimics PI3K pathway activation. Herein, we show that PTEN has a key regulatory function in the development of CLL, as deletion of the *Pten* gene resulted in greatly accelerated onset of the disease. By contrast, deletion of the gene *TP53*, which encodes the tumor suppressor p53 and is highly mutated in CLL, did not accelerate disease development, confirming that development of CLL was specifically triggered by augmented PI3K activity through loss of PTEN and suggesting that CLL driver consequences most likely affect BCR signaling. Moreover, we could show that in human CLL patient samples, 64% and 81% of CLL patients with a mutated and unmutated IgH V_H, respectively, show downregulated PTEN protein expression in CLL B cells if compared to healthy donor B cells. Importantly, we found that B cells derived from CLL patients had higher expression levels of the miRNA-21 and miRNA-29, which suppresses PTEN translation, compared to healthy donors. The high levels of miRNA-29 might be induced by increased PAX5 expression of the B-CLL cells. We hypothesize that downregulation of PTEN by increased expression levels of miR-21, PAX5 and miR-29 could be a novel mechanism of CLL tumorigenesis that is not established yet. Together, our study demonstrates the pivotal role for BCR signaling in CLL development and deepens our understanding of the molecular mechanisms underlying the genesis of CLL and for the development of new treatment strategies.

Introduction

Chronic lymphocytic leukemia (CLL) is the most frequent type of leukemia in Western countries.¹ Like most neoplastic B-cell malignancies, CLL cells maintain their B-cell antigen receptor (BCR) expression.² This selective

pressure to maintain a functional BCR is linked to the fact that malignant B cells profit from the proliferation and survival signals triggered by the BCR.³ Several lines of evidence support a key role of BCR signaling in the pathogenesis of CLL. Thus, CLL with hyper-mutated immunoglobulin heavy chain variable region (IgH V_H) genes

(mutated [M]-CLL) show a more favorable prognosis than those with unmutated IgH V_H genes (unmutated [U]-CLL).⁴ Indeed, patients with fewer than 2% mutations in the IgH V_H genes present a more polyreactive BCR and have a more aggressive disease with shorter survival.⁵ Furthermore, the IgH V_H repertoire is highly restricted leading to different groups of CLL patients with stereotypic BCR.⁶ In contrast to diffuse large B-cell lymphoma (DLBCL), the BCR-activating signaling is not due to mutations in BCR signaling components⁷ but to autonomously activated BCR signaling initiated by the ability of CLL BCR to bind each other.⁸ More recently the crystal structures of a set of CLL BCR identified the regions involved in this binding. Small molecule inhibitors against BTK, like ibrutinib and acalabrutinib show anti-tumor activity in clinical studies of relapsed/refractory CLL.⁹ In line with this, the inhibition of BTK kinase activity through targeted genetic inactivation and inhibition of BTK by ibrutinib in E μ -TCL1 mouse models significantly delays the outbreak of CLL, demonstrating that BCR signaling is critical for CLL development and expansion.¹⁰

The remarkable clinical effectiveness of BCR signaling inhibitors underscores the importance of BCR signaling and of BCR-associated kinases in the proliferation and homing of CLL cells, making this class of agents the treatment of choice for CLL patients.¹¹

The prolonged survival of CLL cells is in part associated with defective apoptosis triggered by the phosphatidylinositol 3-kinase (PI3K)/ protein kinase B (PKB/AKT) and NF- κ B pathways, which, among other pathways, are downstream of the BCR.¹² PI3K exerts its effects by generating phosphatidylinositol-3,4,5-trisphosphate (PI(3,4,5)P3) via phosphorylating the 3-position of the inositol ring of phosphatidylinositol-4,5-bisphosphate (PI(4,5)P2).¹³ On the contrary, the phosphatase and tensin homolog deleted on chromosome 10 (PTEN) can dephosphorylate PI(3,4,5)P3 at the 3-position of the inositol ring converting PI(3,4,5)P3 back to PI(4,5)P2.^{13,14} Loss of PTEN results in accumulation of PI(3,4,5)P3 mimicking the effect of PI3K activation and triggering the activation of its downstream effector AKT.¹⁵ TCL1 is an oncoprotein contributing to occurrence of T-cell prolymphocytic leukemia, as a result of chromosomal translocations and inversions at 14q31.2.¹⁶ Although such a defect is not found in CLL, TCL1 is expressed in more than 90% human CLL patients.¹⁷

In order to facilitate the development of novel therapeutics for B-cell malignancies, an *in vivo* model, which recapitulates the human disease, is required. Several mouse models have provided important insights into CLL pathogenesis.¹⁸ These particularly include the widely studied E μ -TCL1 model.¹⁹ Aging transgenic mice that over-express TCL1 under the control of the μ immunoglobulin (Ig μ) gene enhancer, develop a CD5-positive B-cell lymphoproliferative disorder mimicking human CLL and im-

plicating TCL1 in the pathogenesis of CLL.²⁰ Given the importance of intrinsic BCR signaling in survival and progression of CLL, the establishment of a mouse model that can provide a genetic answer to the importance of the BCR in CLL would be a benefit for the understanding of its pathogenesis.

In this study, we investigated the role of the BCR in the development of a CLL-like B-cell tumor disease in the mouse. The transformed B cells are here referred to as CLL cells. We also explored the impact of the PI3K signaling on the progression of the disease and found that *Pten*-deletion accelerated the onset of leukemogenesis. Moreover, we revealed that PTEN is downregulated in human CLL patients, which might be caused by increased expression levels of the microRNA family miR-29 and the protein PAX5. Thus, by generating inducible mouse models allowing the inactivation of BCR components we established a tool for the investigation of CLL signal transduction and treatment modalities. Our present data identify the BCR as a uniquely important regulator of CLL viability, confirm that an increased PI3K-signaling pathway supports CLL development and maintenance and describe PTEN as a potential target for therapeutic intervention.

Methods

Mouse models

In order to delete the *mb-1* gene, encoding the Ig α protein in B cells, the previously described mouse strain Ig α ^{TMF} (Ig α ^{fl/fl}),²¹ was crossed with the mb1-CreER^{T2} strain (Cd79a^{tm3(cre/ERT2)Reth}), which expresses a tamoxifen-inducible form of the Cre recombinase under the control of the *mb-1* promoter region.²²

Mb1-CreER^{T2}; Ig α ^{fl/fl} mice were crossed to the E μ -TCL1 mouse strain²⁰ to generate the compound mouse mb1-CreER^{T2}; Ig α ^{fl/fl}; E μ -TCL1. The mb1-CreER^{T2}; E μ -TCL1 served as a control.

The *Pten*^{fl/fl} mouse strain²³ was crossed with the mb1-CreER^{T2}; E μ -TCL1. Mice heterozygous for *Pten* (*Pten*^{fl/+}) were generated by crossing *Pten*^{fl/fl} mice²⁴ to the mb1-Cre mouse (Cd79a^{tm1(cre)Reth}/Ehobj) to generate the mb1-Cre; *Pten*^{fl/+} mouse strain. Treatment of the mice with anti-IL7R antibody (Ab) and tamoxifen as well as transfer and propagation of CLL cells in Rag2^{-/-}; γ _c^{-/-} mice is described in the *Online Supplementary Appendix*.

All mice were bred on Black6 background. All animal studies were carried out in accordance with the German Animal Welfare Act, having been reviewed by the regional council and approved under the license (#1288 L1-L18).

Culture of splenic cells

The splenic cells of Tam-treated mb1-CreER^{T2}; *Pten*^{fl/fl}; E μ -TCL1 mice were cultured in complete medium (ISCOVE's,

10% fetal calf serum, 50 mg/mL gentamycin, 50 mM 2-mercapto-ethanol) without any additional growth factors (like BAFF) and incubated at 37°C in the presence of 7.5% CO₂. Only in the case of *ex vivo* inactivation of PTEN expression in purified primary splenic B2 cells from mb1-CreER^{T2};Pten^{fl/fl};Eμ-TCL1 mice and mb1-CreER^{T2};Eμ-TCL1 controls, the cells were cultured in the presence of 50 ng/mL recombinant human BAFF and were treated with 1 μM Tam (4-OHT).

Flow cytometry

For flow cytometric analysis, cell suspensions were pre-treated with α-CD16/CD32 Fc Block (2,4G2; BD Biosciences). Dead cells were excluded by staining with Fixable Viability Dye eFluor 450 (eBioscience). Intracellular (IC) flow cytometry staining was performed using the ADG Fix&Perm Kit (Dianova). The detailed IC and extracellular staining procedure including the respective antibodies is provided in the *Online Supplementary Appendix*. Cells were acquired at a FACS Canto II flow cytometer (BD Biosciences). Analysis was performed using the FlowJo software (Tree Star).

Ca²⁺ influx measurement

0.5–1×10⁶ cells preloaded with the calcium-sensitive fluorescent dye Indo-1 (Invitrogen) were analyzed by flow cytometry (LSR Fortessa, BD Biosciences) upon application of 10 μg/mL anti-IgM F(ab')₂ fragments (Jackson ImmunoResearch).

Chronic lymphocytic leukemia patient and healthy donor sample analysis

CLL samples were obtained from the Department of Internal Medicine III, University Hospital Ulm. Peripheral blood mononuclear cells from healthy donors (HD) were obtained from the Institute for Clinical Transfusion Medicine and Immunogenetics at Ulm University Medical Center. All samples were obtained with informed consent and used in full compliance with institutional regulations (no. 456/19).

Primary CLL patient and HD lymphocytes were isolated from peripheral blood using Ficoll-Paque PLUS (GE Healthcare, 17-440-03). The human samples were MACSed for CD19-positive B cells before microRNA (miRNA) and total RNA isolation for real-time quantitative polymerase chain reaction (qRT-PCR) analysis. More details are provided in the *Online Supplementary Appendix*.

Statistical analysis

Unpaired two-tailed Student's *t*-tests (with *n* between 3 and 5 mice per group) were carried out using Prism 9 software (GraphPad Software Inc) to determine the statistical differences between groups.

Results

Efficient inducible deletion of the Igα-encoding *mb-1* gene in B cells of mb1-CreER^{T2}; Igα^{fl/fl} mice

In order to investigate the efficiency of mb1-CreER^{T2} in the deletion of Igα in mature B cells we crossed mb1-CreER^{T2} with Igα^{fl/fl} mice, in which the exon 3 and 4 of the *mb-1* gene are flanked by *loxP* sites (floxed). All splenic B cells isolated from the tamoxifen (Tam)-treated mb1-CreER^{T2};Igα^{fl/fl} mice lacked both IgM and IgD expression while splenic B cells from the mb1-CreER^{T2} mice treated in the same manner still expressed the BCR (Figure 1A and B). Furthermore, 8 weeks after the start of the Tam-treatment and additional treatment with anti-IL-7R Ab, which block the influx of newly generated B cells from the bone marrow (BM), absolute splenic B-cell numbers from mb1-CreER^{T2};Igα^{fl/fl} mice were significantly reduced (up to 40×) when compared to those from the spleens of the mb1-CreER^{T2} mice (Figure 1C). Additionally, peripheral blood (PBL), lymph nodes (LN) and peritoneal cavity (PC) of these mice contained only a few surviving B cells (Figure 1D). In line with other studies these results demonstrate that mature B cells absolutely require the expression of Igα and consequently of the BCR for their survival in the periphery.

Inactivation of Igα in mouse chronic lymphocytic leukemia reverts the disease phenotype

Although inhibitors against prominent signaling molecules downstream of the BCR, like ibrutinib and idelalisib, successfully eradicate CLL cells in patients, pointing to the quintessential role of the BCR in CLL cell survival, there is no genetic evidence for the involvement of the BCR in the maintenance of CLL cells. Therefore, we generated a mouse model, which enables us to address this question. In order to investigate the role of the BCR in mouse CLL we crossed the mb1-CreER^{T2}; Igα^{fl/fl} mice with the Eμ-TCL1 mouse strain, which is a well-accepted model for mouse CLL, generating mb1-CreER^{T2};Igα^{fl/fl};Eμ-TCL1 mice. Overexpression of TCL1 in B cells drives the development of CLL cells over time. The disease is first detected in 6-month-old mice and its incidence increases with age, reaching its maximum at 12 months. The main features of mouse CLL are the expression of CD5 (Figure 2A; right panel) and the deregulation of B220 and IgD expression. Before and after the beginning of Tam treatment, we assessed the development and survival of CLL cells in the blood of the transgenic mice by flow cytometry using the mouse CLL key markers CD19⁺ CD93⁻ B220^{low} CD5⁺ IgM⁺ IgD⁻. Fully diseased mb1-CreER^{T2};Igα^{fl/fl};Eμ-TCL1 and control mb1-CreER^{T2}; Eμ-TCL1 (12-month-old) carrying mainly CLL cells (Figure 2A) were sacrificed 8 weeks after the beginning of the Tam treatment and without additional treatment with anti-IL-7R Ab. The frequencies and abso-

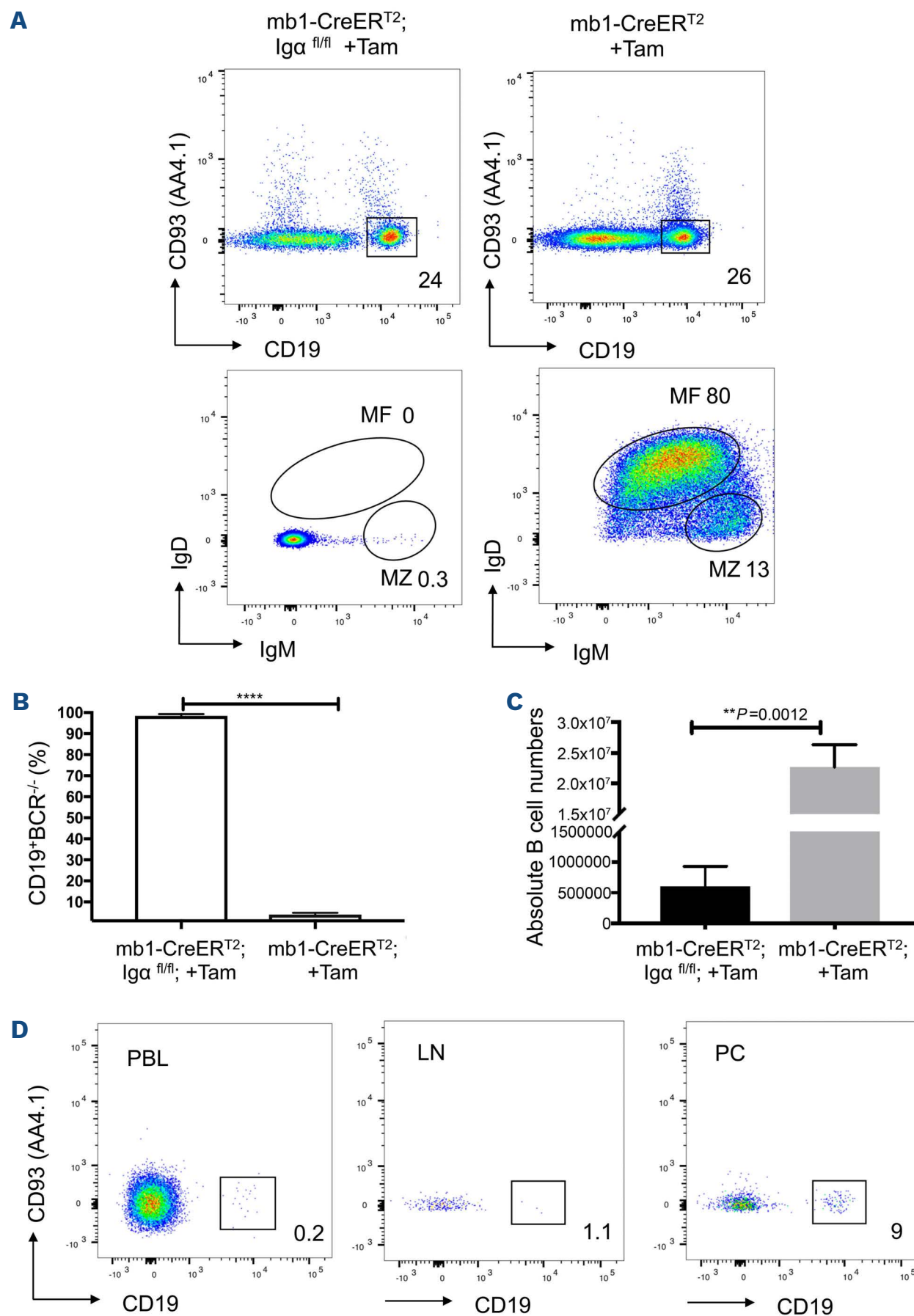


Figure 1. Efficient deletion of the Igα gene leads to the loss of mature B cells. (A) Flow cytometric analysis of B cells from the spleens of mb1-CreER^{T2};Igα^{fl/fl} (left) and mb1-CreER^{T2} control mice (right) treated with tamoxifen (Tam) as described in the Materials and Methods section. Shown are dot plots of the anti-IgM vs. anti-IgD staining after gating on CD19⁺CD93⁻ mature B cells, 2 weeks post Tam treatment. The gated regions in the dot plots correspond to mature follicular (MF) (IgM^{low} IgD^{high}) and marginal zone (MZ) (IgM^{high} IgD^{low}) B cells. The numbers in the dot plots indicate the mean relative frequency of cells in the gate. (B) Quantification of the relative cell count of the Igα-deficient splenic B cells 2 weeks after the beginning of the Tam treatment: bars (left) represent % of cells obtained from mb1-CreER^{T2};Igα^{fl/fl} mice and bars (right) from mb1-CreER^{T2} mice. Graphs are presented as mean ± standard error of the mean (SEM). Four asterisks (****) indicate $P < 0.0001$, P -values were obtained using two-tailed Student's t -test. Cell numbers of 5 mice per group are shown. (C) Statistical analysis of absolute cell numbers of mature splenic B cells 8 weeks after Tam and anti-IL-7R treatment: filled bars represent cells obtained from mb1-CreER^{T2};Igα^{fl/fl} mice and open bars from mb1-CreER^{T2} mice. Two asterisks (**) indicate $P < 0.01$, P -values were obtained using two-tailed Student's t -test. Cell numbers of 5 mice per group are shown. (D) Flow cytometric analysis of B cells peripheral blood (PBL) (left), lymph nodes (LN) (middle) and peritoneal cavity PC (right) of mb1-CreER^{T2};Igα^{fl/fl} mice treated with Tam and anti-IL-7R as described in the Materials and Methods section. Shown are dot plots of the anti-CD19 vs. CD93 staining. The numbers in the dot plots indicate the mean relative frequency of cells in the gate. Data shown are representative of 5 mice.

lute B-CLL cell numbers in the spleen differed dramatically and significantly between mb1-CreER^{T2};Igα^{fl/fl};Eμ-TCL1 and mb1-CreER^{T2};Eμ-TCL1 control mice (Figure 2A and C). The 100-fold decrease of cellularity after deletion of Igα resulted in a significant reduction of the spleen size and weight in mb1-CreER^{T2};Igα^{fl/fl};Eμ-TCL1 mice compared to the Igα-sufficient controls (Figure 2B). In the PBL and the BM (*Online Supplementary Figure S1A to C*), the frequencies and absolute cell numbers of mouse CLL cells differed significantly between mb1-CreER^{T2};Igα^{fl/fl};Eμ-TCL1 and mb1-CreER^{T2};Eμ-TCL1 control mice.

In order to further investigate the impact of Igα gene deletion on the overall survival of the diseased mice, immunodeficient Rag2^{-/-};γ_c^{-/-} mice were intraperitoneally (i.p.) transplanted with splenic cells (1×10⁷) from either mb1-CreER^{T2};Igα^{fl/fl};Eμ-TCL1 or mb1-CreER^{T2};Eμ-TCL1 mice, which were previously sequentially transferred in Rag2^{-/-};γ_c^{-/-}. The mice were treated with Tam three-times every third day, without additional treatment of anti-IL-7R Ab, and were analyzed at day 15 after the start of the treatment. This model has the advantage of producing a CLL-like phenotype including peripheral blood leukemia and splenomegaly in a short period of time, compared to the long period in the original TCL1 model. While Rag2^{-/-};γ_c^{-/-} mice transplanted with mb1-CreER^{T2};Eμ-TCL1 CLL cells died already between day 12 and 18, the mice transplanted with the mb1-CreER^{T2};Igα^{fl/fl};Eμ-TCL1 CLL cells survived up to day 30 (Figure 2D).

Notably, as shown in the previous experiments, BCR-deficient CLL cells of the mb1-CreER^{T2};Igα^{fl/fl};Eμ-TCL1 genotype were significantly reduced in the spleens of the Tam-treated Rag2^{-/-};γ_c^{-/-} mice (Figure 2E and F) as well as in the BM, PC (Figure 2F) and PBL (data not shown), while the CLL cells of the mb1-CreER^{T2};Eμ-TCL1 genotype showed massive accumulation in the spleens and also in the BM and PC (Figure 2F) of the recipient Rag2^{-/-};γ_c^{-/-} mice leading to their early death. Additionally, the spleens from Rag2^{-/-};γ_c^{-/-} mice transplanted with mb1-CreER^{T2};Igα^{fl/fl};Eμ-TCL1-derived CLL cells were smaller compared to the control (*Online Supplementary Figure S1D and E*). Collectively, these findings show that ablation of the BCR in CLL cells is associated with reduced tumor size and increased overall survival demonstrating a clear dependence of CLL cells on BCR.

PI3K activity is reduced in Igα-deficient chronic lymphocytic leukemia cells

PI3K signaling is activated downstream of the BCR and is quintessential for the survival of healthy B cells.²⁵ In order to investigate the effects of BCR deficiency on BCR signaling and the PI3K pathway in CLL cells, we assessed the phosphorylation of the PI3K target AKT and the phosphorylation of other signaling factors downstream of the BCR including LYN, SYK and BTK by intracellular flow cyto-

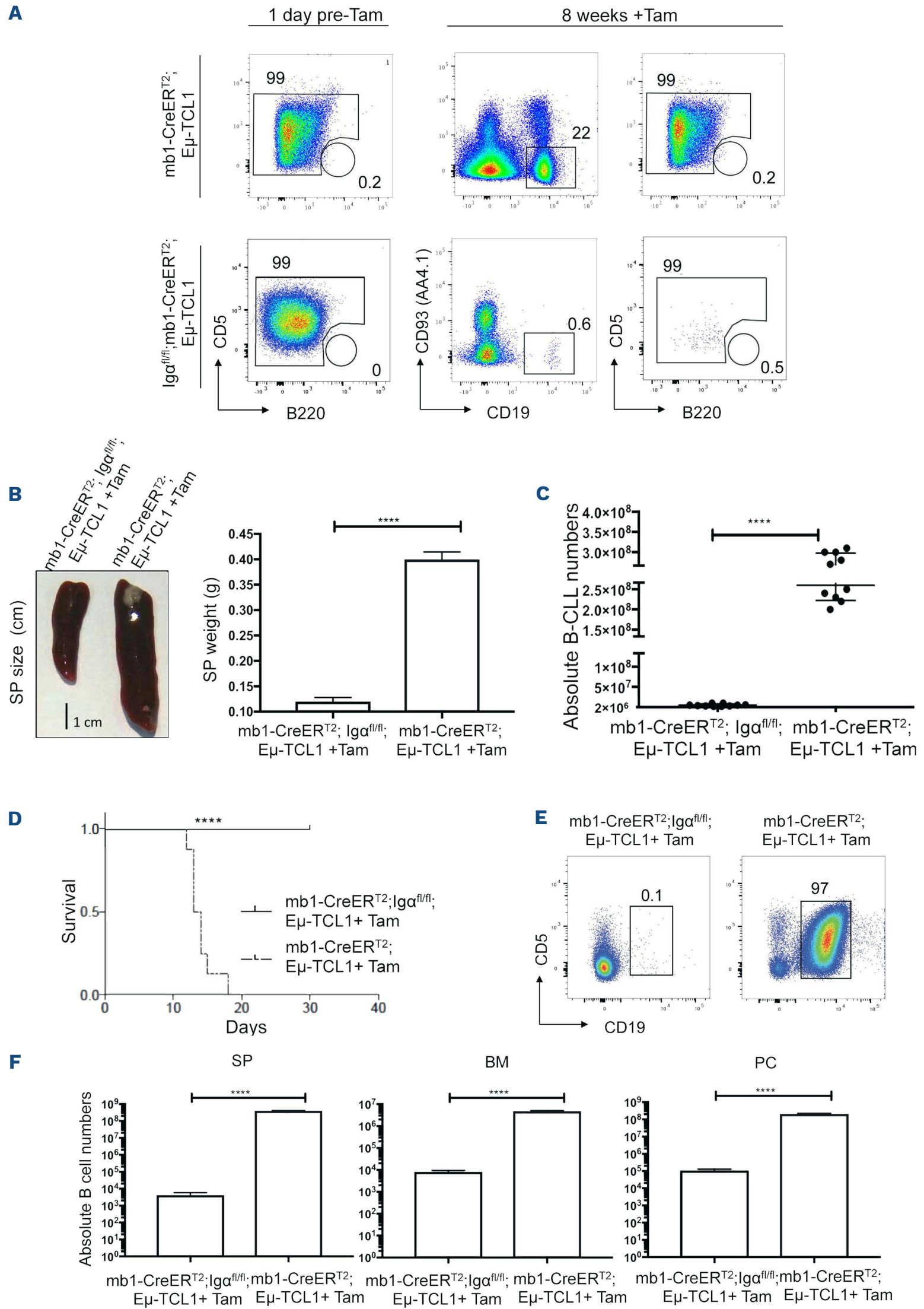
metry in CLL cells 10 days after induced Igα deletion. The time point of 10 days was selected, because we already observed a complete loss of Igα and BCR expression at this time but enough cells for flow cytometric analysis were still alive. Ten days after induced Igα deletion, the BCR-deficient CLL cells showed decreased AKT phosphorylation at S473 and T308 compared to the BCR-sufficient CLL control cells as well as significantly reduced LYN phosphorylation (Y396/Y507), SYK phosphorylation (Y525/526) and BTK phosphorylation (Y223) (Figure 3A and B). In addition, we analyzed whether the CLL cells could be stimulated by IgM F(ab')₂ treatment after Igα deletion. Using a calcium influx assay, we observed that, in contrast to mb1-CreER^{T2};Eμ-TCL1 CLL control cells, CLL cells from mb1-CreER^{T2};Igα^{fl/fl};Eμ-TCL1 mice did not release Ca²⁺ upon BCR stimulation with IgM F(ab')₂ fragments 10 days after Tam treatment (Figure 3E). Moreover, 5 minutes after stimulation with anti-IgM F(ab')₂ fragments, the Igα-deficient CLL cells show less increase of SYK-phosphorylation at Y525 and Y526 compared to mb1-CreER^{T2};Eμ-TCL1 CLL control cells (*Online Supplementary Figure S2G*).

The decrease in AKT phosphorylation after Igα deletion points to a reduced PI3K activity in the absence of the BCR. Moreover, the decreased phosphorylation of the BCR-proximal kinases LYN, SYK and BTK indicates that BCR signaling is downregulated in CLL B cells in consequence of Igα deletion. Constitutively active PI3K signaling may lead to increased BCL-2 expression.²⁶ Therefore, we investigated the expression of BCL-2 in BCR-deficient and BCR-expressing B cells. BCR-deficient CLL cells from mb1-CreER^{T2};Igα^{fl/fl};Eμ-TCL1 had significantly decreased BCL-2 expression 10 days after Tam treatment as compared to control cells (Figure 3C and D). In line with this, we observed a slight downregulation of the anti-apoptotic protein myeloid cell leukemia sequence 1 (MCL-1) in CLL cells 10 days after induced Igα deletion (*Online Supplementary Figure S2A and F*; left). Considering that BCL-2 is also regulated by NFκB, we tested whether ablation of the BCR in CLL cells from mb1-CreER^{T2};Igα^{fl/fl};Eμ-TCL1 mice also resulted in reduced NFκB activity by analyzing IKKα/β phosphorylation at S176/180 and phosphorylation of NFκB p65 at S536 10 days after induced Igα deletion. Interestingly, our analysis revealed that IKKα/β phosphorylation at S176/180, phosphorylation of NFκB p65 at S536 and thus NFκB activity is slightly downregulated in CLL cells with induced Igα deletion compared to Eμ-TCL1 CLL control cells (*Online Supplementary Figure S2B, C and F*).

Together, these data suggest that BCR-mediated activation of PI3K signaling is essential for the survival of CLL B cells and that reduced NFκB activity and BCL-2 upregulation may be an important part of this regulation.

PTEN-loss augments PI3K activity and results in early onset of chronic lymphocytic leukemia

Next, we explored the role of the PI3K signaling pathway



Continued on following page.

Figure 2. The B-cell antigen receptor (BCR) is indispensable for the survival of mouse chronic lymphocytic leukemia cells and inactivation of the BCR prolongs the survival of adoptive transfer recipient mice. (A) Flow cytometric analysis of B cells from the spleens of mb1-CreER^{T2};E μ -TCL1 control mice and mb1-CreER^{T2};I γ $\alpha^{fl/fl}$;E μ -TCL1 mice before and 8 weeks after tamoxifen (Tam) treatment. Shown are dot plots of the anti-B220 vs. anti-CD5 staining after gating on CD19⁺ CD93⁻ B cells (gating shown). The gated regions in the anti-B220 vs. anti-CD5 dot plots correspond to chronic lymphocytic leukemia (CLL) cells (CD19⁺ CD93⁻ B220^{low} CD5⁺ IgM⁺ IgD⁻) and mature healthy B cells (CD19⁺ CD93⁻ B220⁺ CD5⁻ IgM⁺ IgD⁺). The numbers in the dot plots indicate the mean relative frequency of cells in the gate. (B) Spleen (SP) pictures (left) and quantification of the SP weight (right) obtained from mb1-CreER^{T2};I γ $\alpha^{fl/fl}$;E μ -TCL1 mice and mb1-CreER^{T2};E μ -TCL1 control mice 8 weeks after the beginning of the Tam treatment (left). The graphs (right) are presented as mean \pm standard error of the mean (SEM). Four asterisks (****) indicate $P < 0.0001$, P -values were obtained using two-tailed Student's t -test. Cell numbers of 5 mice per group are shown (right). (C) Statistical analysis of absolute cell numbers of CLL cells 8 weeks after Tam treatment: filled circles indicating cells obtained from mb1-CreER^{T2};I γ $\alpha^{fl/fl}$;E μ -TCL1 mice (left) and from mb1-CreER^{T2};E μ -TCL1 mice (right). Four asterisks (****) indicate $P < 0.0001$, P -values were obtained using two-tailed Student's t -test. Cell numbers of 10 mice per group are shown with each circle representing an individual animal. (D) Kaplan-Meier survival curve showing the survival of recipient Rag2^{-/-}; $\gamma_c^{-/-}$ mice transferred with 10⁷ splenic CLL-like B cells derived from the mb1-CreER^{T2};E μ -TCL1 control or the mb1-CreER^{T2};I γ $\alpha^{fl/fl}$ mice and treated with Tam at day 3 post transfer. Every point represents an individual mouse with $n=10$. The P -value ($P < 0.0001$) was determined by Mantel-Cox log-rank test. (E) Flow cytometric analysis of B cells from SP of Rag2^{-/-}; $\gamma_c^{-/-}$ mice derived from the mb1-CreER^{T2};I γ $\alpha^{fl/fl}$;E μ -TCL1 (left) and the mb1-CreER^{T2};E μ -TCL1 (right) mice +Tam. Shown are dot plots of the anti-CD19 vs. anti-CD5 staining at day 10 post transfer. The gated regions in the dot plots correspond to the individual B-cell populations. The numbers in the dot plots indicate the mean relative frequency of cells in the gate. (F) Statistical analysis of absolute cell numbers from SP (left), bone marrow (BM, middle) and peritoneal cavity (PC, right) of Rag2^{-/-}; $\gamma_c^{-/-}$ mice transplanted with mb1-CreER^{T2};I γ $\alpha^{fl/fl}$;E μ -TCL1 (left bar) or mb1-CreER^{T2};E μ -TCL1 (right bar) mouse CLL B cells. Graphs are presented as mean \pm SEM. Four asterisks (****) indicate $P < 0.0001$, P -values were obtained using two-tailed Student's t -test. Cell numbers of 5 mice per group are shown.

in the onset and maintenance of mouse CLL by inactivating PTEN, the negative regulator of the PI3K signaling pathway. To this end, we generated a mouse model with a B cell-specific and Tam-induced deletion of the *Pten* gene. In order to investigate the role of PTEN in the onset of mouse-CLL, we crossed the mb1-CreER^{T2};E μ -TCL1 mice to the *Pten*^{fl/fl} mouse strain to generate mb1-CreER^{T2};Pten^{fl/fl};E μ -TCL1 mice. These mice were treated with Tam at a young age (6 weeks) before the detection of any CLL B cells in the peripheral blood or the outbreak of mouse CLL that are usually evident at 3 to 6 months in mb1-CreER^{T2};Pten^{fl/fl};E μ -TCL1 and mb1-CreER^{T2};E μ -TCL1 mice, respectively. We assessed the development of CLL cells using the mouse CLL key markers CD19⁺ B220^{low} CD5⁺ IgM⁺ IgD⁻. mb1-CreER^{T2};E μ -TCL1 mice served as controls. Eight and 16 weeks after the beginning of the Tam treatment the mice were analyzed by flow cytometry for the absolute cell number of CD19⁺ B220^{low} CD5⁺ IgM⁺ IgD⁻ B cells. At both time points the number of CLL cells was increased (8 weeks: $>2 \times 10^6$, Figure 4A; 16 weeks: $>2 \times 10^7$, Figure 4B) in the mb1-CreER^{T2};Pten^{fl/fl};E μ -TCL1 mice as compared to those from the spleens of the mb1-CreER^{T2};E μ -TCL1 control mice. These data show that after loss of PTEN, the resulting constitutive activity of the PI3K pathway leads to accelerated development of CLL in young mice as shown by the accumulation of CLL B cells with time. Recent studies reported that either germline deletion²⁷ or insertion of a single mutation²⁸ in the *Tp53* gene (encoding the tumor suppressor p53), a gene, which is often mutated in CLL,²⁹ on E μ -TCL1 background also accelerated the development of the CLL disease. We deleted the *Tp53* gene in mb1-CreER^{T2};E μ -TCL1 mice and found out that 24 weeks post treatment 94 % of B cells in the spleens of the mb1-CreER^{T2};Pten^{fl/fl};E μ -TCL1 mice became

CLL cells, whereas the mb1-CreER^{T2};Tp53^{fl/fl};E μ -TCL1 mice showed 2% of CLL cells (Figure 4C). By assessing the expression of p53 by flow cytometry we confirmed that *Tp53* was indeed deleted in mb1-CreER^{T2};Tp53^{fl/fl};E μ -TCL1 mice (Figure 4D). In addition, we compared the development of CLL in mice lacking *Tp53* expression (mb1-Cre;Tp53^{fl/fl};E μ -TCL1) to mice with a constitutive heterozygous loss of *Pten* (mb1-Cre;Pten^{fl/+};E μ -TCL1). At 32 weeks, the mb1-Cre;Pten^{fl/+};E μ -TCL1 mice showed 94% of CLL cells whereas mb1-Cre;Tp53^{fl/fl};E μ -TCL1 mice developed only 27% of CLL B cells in the blood (Figure 4E). Moreover, a combined deletion of *Tp53* and *Pten* in mb1-Cre;Pten^{fl/+};Tp53^{fl/fl};E μ -TCL1 mice did not accelerate the outbreak of CLL when compared to mb1-Cre;Pten^{fl/+};E μ -TCL1 mice (Online Supplementary Figure S3A). This confirms that the accelerated development of the disease is specifically driven by the partial loss of PTEN and the subsequent activation of the PI3K pathway.

As further signs of elevated PI3K signaling, we found an increased phosphorylation of S473 of AKT and Y223 of BTK in CD19⁺ B220^{low} CD5⁺ IgM⁺ IgD⁻ CLL cells from the spleens of mb1-CreER^{T2};Pten^{fl/fl};E μ -TCL1 mice compared to CLL cells from the mb1-CreER^{T2};E μ -TCL1 control mice (Figure 4F; Online Supplementary Figure S3 D and E). In order to investigate, whether PTEN deficiency resulted in constitutive activation of the PI3K/AKT pathway, we stimulated splenic CLL cells from mb1-CreER^{T2};Pten^{fl/fl};E μ -TCL1 mice and mb1-CreER^{T2};E μ -TCL1 control mice with anti-IgM F(ab')₂ fragments and monitored the AKT phosphorylation at S473 and T308 as well as BTK phosphorylation at Y223 after 5 minutes of stimulation. In both cases, we could not observe any significant increase in phosphorylation after BCR stimulation indicating that both, wild-type TCL1 leukemia cells and PTEN-deficient leukemia cells exhibit

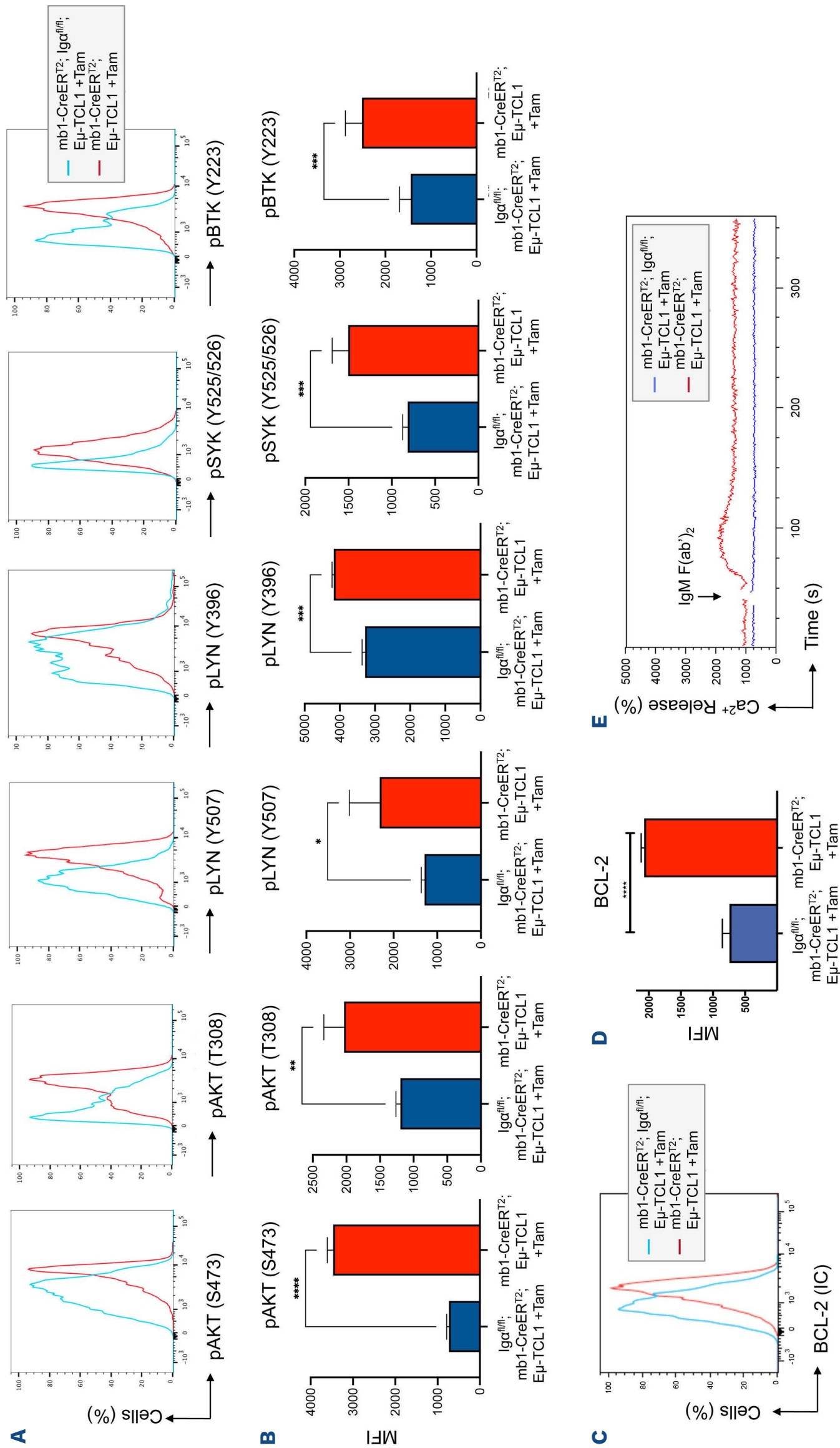


Figure 3. AKT phosphorylation and BCL-2 expression are reduced in Igα-deficient chronic lymphocytic leukemia cells. (A) Flow cytometric analysis of AKT phosphorylation (S473 and (T308), LYN phosphorylation (Y396) and (Y507), SYK phosphorylation (Y525/526), BTK phosphorylation (Y223) on splenic chronic lymphocytic leukemia (CLL) cells from tamoxifen (Tam)-treated mice (day 10): mb1-CreER^{T2};Eμ-TCL1 (red line) and mb1-CreER^{T2};Igα^{fl/fl};Eμ-TCL1 (blue line). (B) Quantification of the intracellular mean fluorescence intensity (MFI) in splenic mouse CLL B cells from mb1-CreER^{T2};Igα^{fl/fl};Eμ-TCL1 (blue filled bars) and mb1-CreER^{T2};Eμ-TCL1 (red filled bars) mice. MFI of AKT phosphorylation (S473 and (T308), LYN phosphorylation (Y396) and (Y507), SYK phosphorylation (Y525/526) and BTK phosphorylation (Y223) are shown. Graphs are presented as mean ± standard error of the mean (SEM). *P*-values were obtained using the two-tailed Student's *t*-test (***P*<0.01; ****P*<0.001; *****P*<0.0001). Results from 5 mice per group are shown. (C) Flow cytometric analysis of BCL-2 expression on splenic CLL cells from Tam-treated mice (day 10): mb1-CreER^{T2};Eμ-TCL1 (red line) and mb1-CreER^{T2};Igα^{fl/fl};Eμ-TCL1 (blue line). (D) Quantification of the intracellular BCL-2 MFI in splenic mouse CLL B cells from mb1-CreER^{T2};Eμ-TCL1 (red filled bars) and mb1-CreER^{T2};Igα^{fl/fl};Eμ-TCL1 (blue filled bars) mice. Graphs are presented as mean ± SEM. Four asterisks (****) indicate *P*<0.0001, *P*-values were obtained using two-tailed Student's *t*-test. Results from five mice per group are shown. (E) Flow cytometric analysis of the intracellular Ca²⁺ influx mature splenic B cells from the Tam-treated mb1-CreER^{T2};Igα^{fl/fl};Eμ-TCL1 (blue line) and mb1-CreER^{T2};Eμ-TCL1 (red line) after treatment with 10 μg/mL anti-IgM F(ab')₂ fragments. Data shown are representative of 3 independent experiments.

a constitutive active PI3K/AKT signaling, that cannot be significantly increased by BCR stimulation (*Online Supplementary Figure S3B and C*).

Additionally, BCL-2 expression was higher in PTEN-deficient CD19⁺ B220^{low} CD5⁺ IgM⁺ IgD⁻ cells relative to the control (Figure 4F, right; *Online Supplementary Figure S3F*). Statistical analysis confirmed that the increased AKT- and BTK-phosphorylation as well as the increased BCL-2 expression in the PTEN-deficient CLL B cells was significant compared to the PTEN-sufficient control (Figure 4F). Furthermore, we affirmed by flow cytometry that the *Pten* gene was efficiently deleted in splenic CLL cells from mb1-CreER^{T2};Pten^{fl/fl};Eμ-TCL1 mice and mb1-CreER^{T2};Eμ-TCL1-derived cells served as a control (*Online Supplementary Figure S3G*). In conclusion, in the absence of PTEN, the CLL cells exhibit significant increase in AKT and BTK phosphorylation likely leading to higher activity of these molecules. These findings provide evidence for enhanced PI3K signaling in these PTEN-deficient cells. Furthermore, in this model, conditional inactivation of PTEN resulted in the accelerated onset of CLL.

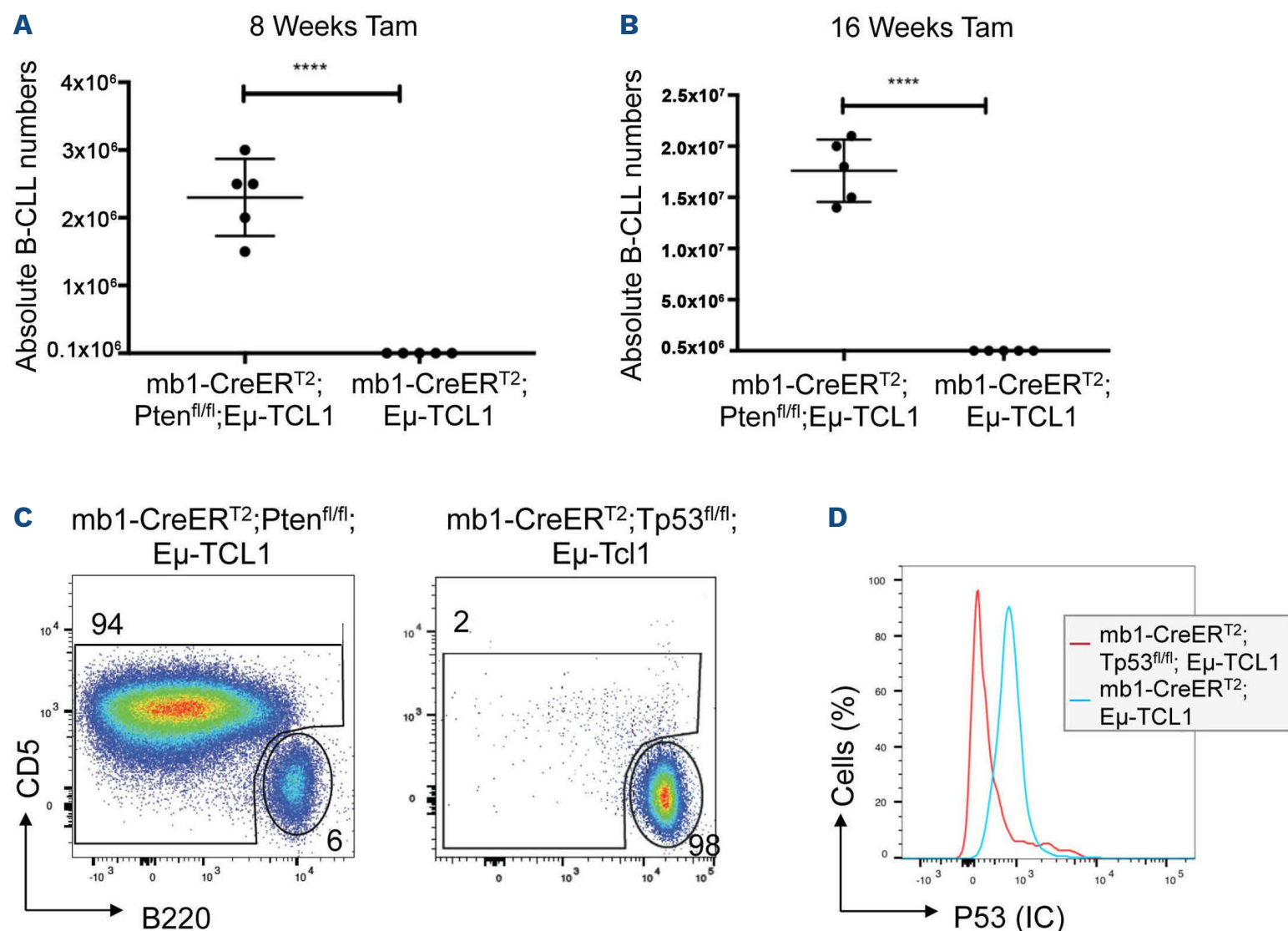
Deletion of *Pten* leads to autonomous survival of chronic lymphocytic leukemia cells

In order to test the tumorigenic potential of the primary

splenic CD19⁺ B220^{low} CD5⁺ IgM⁺ IgD⁻ PTEN-deficient CLL cells from Tam-treated mb1-CreER^{T2};Pten^{fl/fl};Eμ-TCL1 mice, we transferred them into Rag2^{-/-};γ_c^{-/-} mice. Two weeks post engraftment, a population of CD19⁺ B220^{low} CD5⁺ IgM⁺ IgD⁻ cells was detected in the spleen (Figure 5A).

Surprisingly, the primary splenic PTEN-deficient CLL cells from Tam-treated mb1-CreER^{T2};Pten^{fl/fl};Eμ-TCL1 mice grew autonomously in culture and preserved the features of mouse CLL cells retaining their CD19⁺ B220^{low} CD5⁺ IgM⁺ IgD⁻ phenotype. The cells were cultured in a medium supplemented only with fetal calf serum and in the absence of any additional growth factors or antigen (Figure 5B). The PTEN deficiency of these cell lines was confirmed by genotyping and flow cytometry (Figure 5C; *Online Supplementary Figure S4A*, right). We generated five different CLL-like cell lines, which were heterogenous, but grew similarly in culture over prolonged period of time without growth factor supplements.

After growing in culture for 4 months, functional analysis revealed that some of these cell lines mobilized intracellular Ca²⁺ release upon stimulation with a polyclonal anti-IgM F(ab')₂ antibody (Figure 5D). CD19⁺ B220^{low} CD5⁺ IgM⁺ IgD⁻ CLL cells phenotypically resemble B-1 B cells. Since BCR of some B1 B cells are specific to phosphatidyl choline (Ptc), we assessed by flow cytometry whether the



Continued on following page.

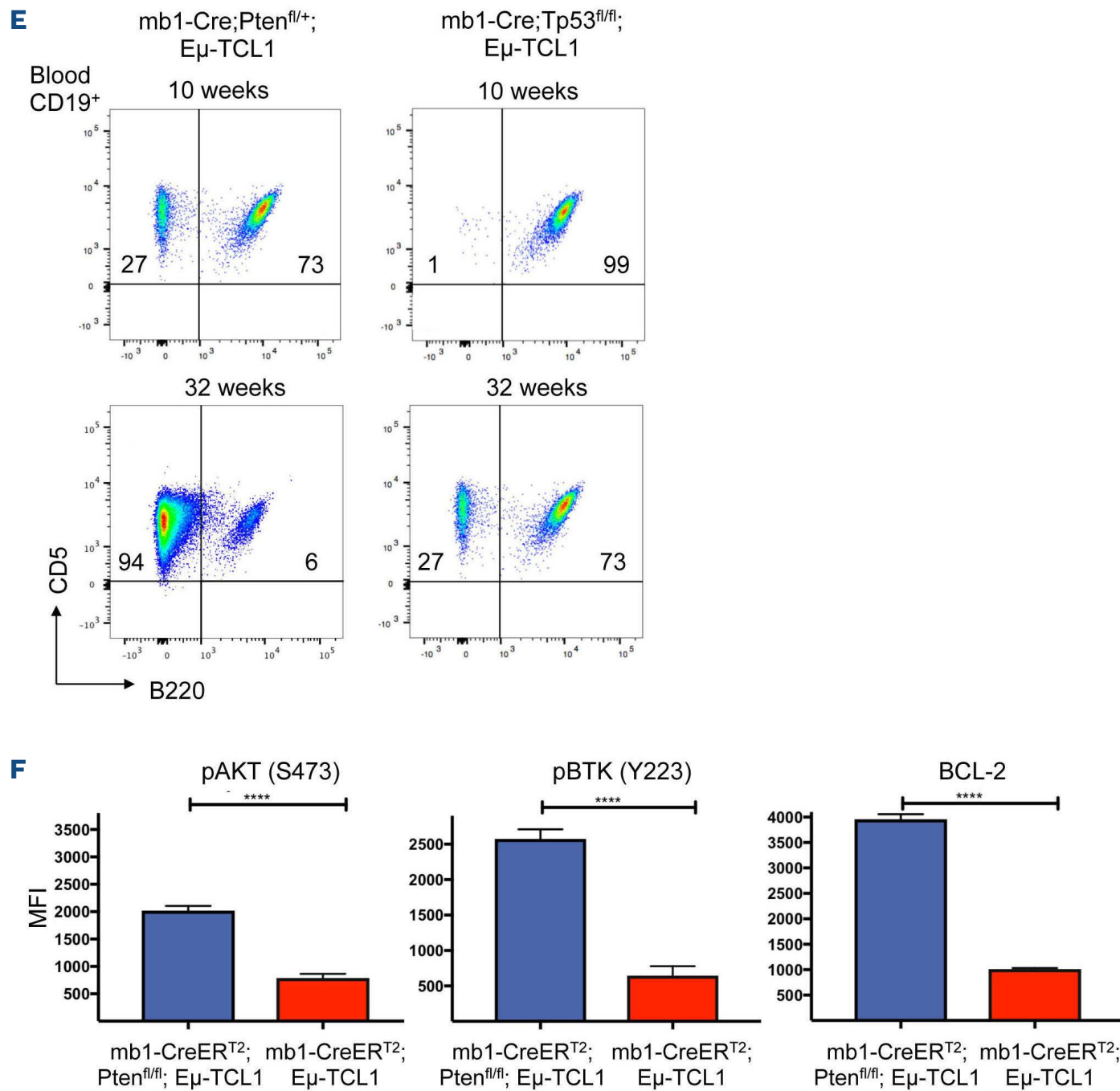


Figure 4. Deletion of *Pten* but not *Tp53* leads to accelerated mouse chronic lymphocytic leukemia. (A and B) Statistical analysis of absolute cell numbers of chronic lymphocytic leukemia (CLL) cells (CD19⁺ B220^{low} CD5⁺) (A) 8 weeks and (B) 16 weeks after tamoxifen (Tam) treatment of 6-week-old mice: filled circles indicating cells obtained from mb1-CreER^{T2};Pten^{fl/fl};Eμ-TCL1 mice (left) and from mb1-CreER^{T2};Eμ-TCL1 mice (right). Four asterisks (****) indicate $P < 0.0001$, P -values were obtained using two-tailed Student's t -test. Cell numbers from 5 mice per group are shown with each circle representing an individual animal. (C) Flow cytometric analysis of B cells from the spleens of mb1-CreER^{T2};Pten^{fl/fl};Eμ-TCL1 (left), and mb1-CreER^{T2};Tp53^{fl/fl};Eμ-TCL1 (right) 24 weeks after Tam treatment of 6-week-old mice. Shown are dot plots of the anti-B220 vs. anti-CD5 staining after gating on CD19⁺ B cells. The gated regions in the dot plots correspond to CLL cells (CD19⁺ B220^{low} CD5⁺) and healthy B cells (CD19⁺ B220^{high} CD5⁻). The numbers in the dot plots indicate the mean relative frequency of cells in the gate. (D) Flow cytometric analysis of p53-expression in splenic CLL cells from Tam-treated mb1-CreER^{T2};Tp53^{fl/fl};Eμ-TCL1 mice (red line) and splenic CLL cells from mb1-CreER^{T2};Eμ-TCL1 mice (blue line). (E) Flow cytometric analysis of B cells isolated from the blood of mb1-Cre;Pten^{fl/fl};Eμ-TCL1 and mb1-Cre;Tp53^{fl/fl};Eμ-TCL1 mice at the age of 10 weeks and 32 weeks. The graph shows dot-plots of the anti-B220 vs. anti-CD5 staining after gating on viable CD19⁺ B lymphocytes. The numbers in the dot plots indicate the mean relative frequency of cells in the gate. (F) Quantification of p-AKT (left) and p-BTK (middle), and BCL-2 (right) mean fluorescence intensity (MFI) in splenic mouse CLL B cells from mb1-CreER^{T2};Pten^{fl/fl};Eμ-TCL1 (blue filled bars) and mb1-CreER^{T2};Eμ-TCL1 (red filled bars) mice. Mean \pm standard deviation are shown. Four asterisks (****) indicate $P < 0.0001$, P -values were obtained using two-tailed Student's t -test. Results from 5 mice per group are shown.

CLL-like CreER^{T2};Pten^{fl/fl};Eμ-TCL1 cells were capable of binding Ptc liposomes. We found that some PTEN-deficient CLL-like cell lines could not bind Ptc with their BCR (Online Supplementary Figure S4A, blue line) as compared to PTEN-sufficient CLL-like CreER^{T2};Eμ-TCL1 control cells (Online Supplementary Figure S4A, red line). In addition, we concluded that PTEN-deficient CLL-like cell lines were

polyclonal because we detected multiple V_β-J_β recombination events within one population (Online Supplementary Figure S4B). Taken together, constitutive activation of PI3K signaling through loss of PTEN accelerates CLL development and allows efficient engraftment and maintenance of CLL-like B cell *in vivo* and *in vitro*. Because BCL-2 expression was increased in splenic PTEN-

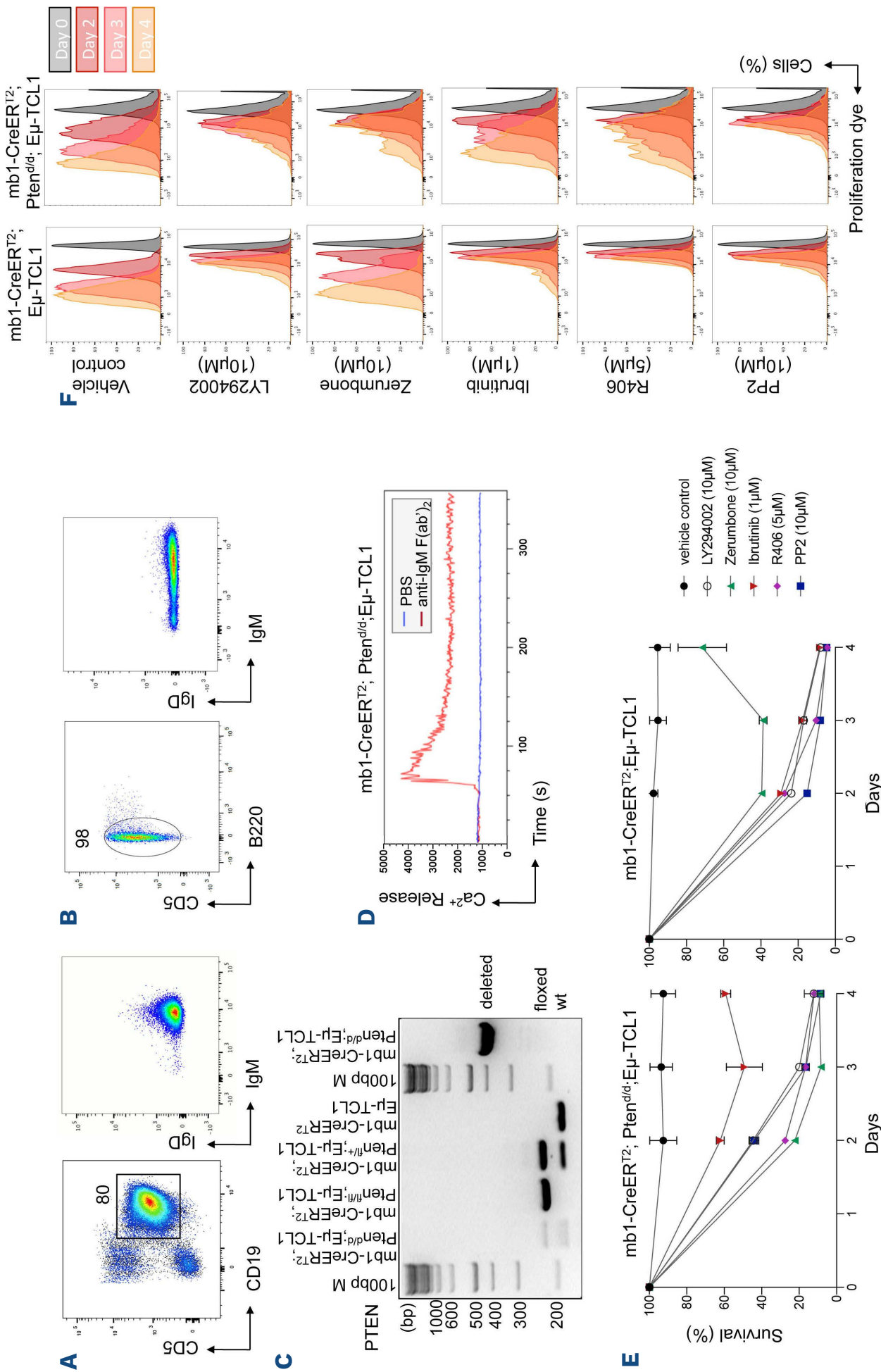


Figure 5. Deletion of *Pten* leads to autonomous survival of chronic lymphocytic leukemia B cells ex vivo. (A) Flow cytometric analysis of B cells from the spleens of Rag2^{-/-}; γ_c^{-/-} mice transplanted with splenic B cells from mb1-CreER^{T2}; Pten^{fl/fl}; Eμ-TCL1 derived from the experiment depicted in (Figure 4C, left). Dot plot of the anti-CD19 vs. anti-CD5 (left) and anti-IgD vs. anti-IgM (right) staining is shown. (B) Flow cytometric analysis of B cells from the spleens of mb1-CreER^{T2}; Pten^{fl/fl}; Eμ-TCL1 cultured ex vivo. Dot plots of the anti-B220 vs. anti-CD5 (left) and anti-IgD (right) staining after gating on CD19⁺ B220^{low} CD5⁺ and healthy mature B cells (CD19⁺ CD5⁺) correspond to chronic lymphocytic leukemia (CLL) cells (CD19⁺ B220^{low} CD5⁺) and healthy mature B cells (CD19⁺ B220⁺ CD5⁻). The numbers in the dot plots indicate the mean relative frequency of cells in the gate. (C) Analysis of the *Pten* locus recombination in genomic DNA (gDNA) from the mb1-CreER^{T2}; Pten^{d/d}; Eμ-TCL1 cells in comparison to mb1-CreER^{T2}; Pten^{fl/fl}; Eμ-TCL1, mb1-CreER^{T2}; Pten^{fl/+}; Eμ-TCL1, and mb1-CreER^{T2}; Eμ-TCL1. Left panel: floxed (fl) and wt (+) alleles. Right panel: the recombinant deleted (d) allele. (D) Flow cytometric analysis of the intracellular Ca²⁺ influx in cultured splenic cells from the tamoxifen (Tam)-treated mb1-CreER^{T2}; Pten^{fl/fl}; Eμ-TCL1. Cells were treated with 10 μg/mL anti-IgM F(ab)₂ fragments (red line) or left untreated (blue line). Data shown are representative of 3 independent experiments. (E) Survival plot of mb1-CreER^{T2}; Pten^{d/d}; Eμ-TCL1 (left) and mb1-CreER^{T2}; Eμ-TCL1 (right) chronic lymphocytic leukemia (CLL)-like culture cells after treating the cells for 4 days with the vehicle control (dimethyl sulfoxide [DMSO]; black) or the inhibitors LY294002 (10 μM; white), zerumbone (10 μM, green), ibrutinib (1μM; red), R406 (5 μM; pink) and PP2 (10 μM; blue). Graphs are presented as mean ± standard error of the mean; dots indicate the percentage of survived cells normalized to vehicle control (100%). Three technical replicates per group are shown. (F) Flow cytometric analysis of proliferation dye intensity of labeled mb1-CreER^{T2}; Pten^{d/d}; Eμ-TCL1 and mb1-CreER^{T2}; Eμ-TCL1 culture cells at day 0 (black), day 2 (dark red), day 3 (red), day 4 (orange) after treatment with the inhibitors LY294002 (10 μM), zerumbone (10 μM), ibrutinib (1 μM), R406 (5 μM) and PP2 (10 μM).

deficient CLL cells from mb1-CreER^{T2};Pten^{fl/fl};Eμ-TCL1 mice, we treated the cells cultured for 4 months with the BCL-2 inhibitor ABT-199 (also known as venetoclax). The relative numbers of the PTEN-deficient as well as PTEN-sufficient cells were 5-fold decreased at a concentration of 10 μM compared to the vehicle (dimethyl sulfoxide [DMSO]) control (*Online Supplementary Figure S4C*).

Moreover, in order to test whether the PTEN-deficient CLL-like cells in culture were still dependent on BCR signaling for survival and proliferation, we treated the cells with inhibitors blocking BCR downstream signaling and assessed the survival and proliferation of the cells in culture for 4 days. We used LY294002 (10 μM) as a selective PI3K inhibitor, zerumbone (10 μM) to block NFκB activity, ibrutinib (1 μM) to inhibit BTK activity, R406 (5 μM) as a SYK inhibitor and PP2 (10 μM) to block Src-family tyrosine kinases. All of the inhibitors significantly reduced the survival and proliferation of both mb1-CreER^{T2};Pten^{d/d};Eμ-TCL1 and mb1-CreER^{T2};Eμ-TCL1 culture cells when compared to the cells treated with vehicle control (DMSO) (Figure 5E and F). This indicates that the PTEN-deficient cells that are autonomously growing in culture are still dependent on BCR signaling and the activity of NFκB. Interestingly, we observed higher survival and proliferation of *Pten*-deleted CLL-like cells treated with inhibitors blocking BCR signaling (LY294002, ibrutinib, R406, PP2) when compared to the treated mb1-CreER^{T2};Eμ-TCL1 leukemic cells (*Online Supplementary Figure S4D and E*). *Vice versa*, mb1-CreER^{T2};Eμ-TCL1 cells treated with the NFκB inhibitor zerumbone showed better survival and proliferation when compared to the PTEN-deficient mb1-CreER^{T2};Pten^{d/d};Eμ-TCL1 culture cells (*Online Supplementary Figure S4D and E*).

In order to test whether the CD19⁺ B220^{low} CD5⁺ IgM⁺ IgD⁻ CLL cells could be generated if *Pten* was deleted *ex vivo* on Eμ-TCL1 background, we treated purified primary splenic B2 cells from mb1-CreER^{T2};Pten^{fl/fl};Eμ-TCL1 mice and mb1-CreER^{T2};Eμ-TCL1 controls with Tam (4-OHT) in culture in the presence of the B-cell activating factor (BAFF). The *ex vivo*-generated PTEN-deficient CLL cells were more abundant compared to the PTEN-sufficient control (26% to 8%) (*Online Supplementary Figure S5A and B*). However, these cells could not survive for an extended time period in culture.

Heterozygous loss of *Pten* accelerates chronic lymphocytic leukemia development

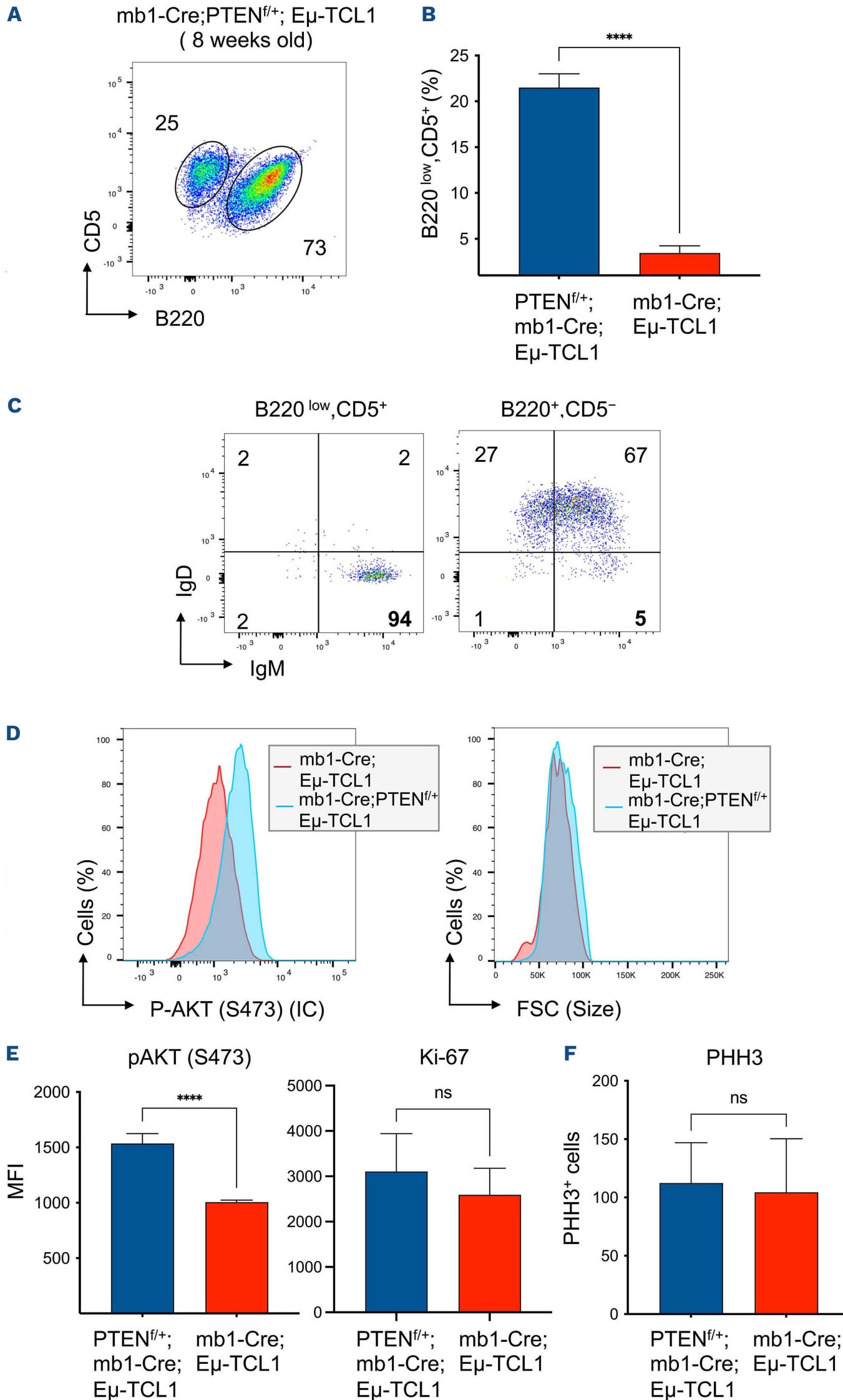
In order to strengthen the evidence that PTEN-deficiency and subsequent enhanced PI3K-activity, monitored by AKT-phosphorylation, lead to accelerated onset of mouse CLL, we intercrossed the mb1-Cre;Eμ-TCL1 with the Pten^{fl/+} strains to generate the mb1-Cre; Pten^{fl/+};Eμ-TCL1 which allows for a constitutive heterozygous deletion of the *Pten* gene in B cells. Only one “floxed” *Pten* allele was introduced because constitutive *Pten* deletion on both al-

leles leads to a block of B-cell development at the pro-B-cell stage due to the inability to express a μHC.³⁰

In these mice, we detected an early development of CLL cells at 8 weeks of age (Figure 6A). This was supported by the quantification of five independent experiments with five individual mice each showing that CLL cells accumulated in the spleens of young (8 weeks old) mb1-Cre;Pten^{fl/+};Eμ-TCL1 mice (Figure 6B, blue bar) but not in control mb1-Cre;Eμ-TCL1 mice (Figure 6B, red bar). The CD19⁺ B220^{low} CD5⁺ CLL cells expressed only IgM and no IgD (Figure 6C, left) as compared to the CD19⁺ B220⁺ CD5⁻ cell population (IgM⁺ IgD⁺) from the same mice (Figure 6C, right). Consistent with the heterozygous loss of *Pten*, the splenic CD19⁺ B220^{low} CD5⁺ IgM⁺ IgD⁻ CLL cells from mb1-Cre;Pten^{fl/+};Eμ-TCL1 displayed significantly more AKT phosphorylation than splenic B cells from the mb1-Cre;Eμ-TCL1 mice (Figure 6D and E, left). Together, these results indicate that the constitutive loss of one *Pten* allele in combination with overexpression of TCL1 significantly accelerates the onset of CLL.

Heterozygous *Pten* deletion does not lead to Richter's transformation

It was recently shown by Kohlhaas *et al.* that constitutive activation of AKT in Eμ-TCL1 mice results in Richter's transformation (RT), an aggressive lymphoma which occurs upon progression from CLL.³¹ So, we investigated if mb1-Cre;Pten^{fl/+};Eμ-TCL1 mice with a heterozygous *Pten* deletion develop RT and histologically analyzed spleens from diseased mice for features of RT. RT cells can be distinguished from CLL cells by morphological abnormalities, large lymphoid cells and increased proliferation. Histone H3 phosphorylation on S10 is specific to mitosis and phosphorylated histone H3 (PHH3) proliferation markers are increasingly being used to evaluate proliferation in various tumors.³² Therefore, we analyzed the number of PHH3-positive cells in spleens of diseased mb1-Cre;Pten^{fl/+};Eμ-TCL1 and mb1-Cre;Eμ-TCL1 control mice by fluorescence microscopy. However, no significant difference in PHH3 positive cells could be observed (Figure 6F; *Online Supplementary Figure S5C*) as well as no difference in size of the CLL cells (*Online Supplementary Figure S5E*). Hematoxylin and eosin (H&E) staining on paraffin embedded splenic sections of diseased mb1-Cre;Pten^{fl/+};Eμ-TCL1 and mb1-Cre;Eμ-TCL1 mice also revealed no significant changes after *Pten* deletion in splenic CLL cells (*Online Supplementary Figure S5D*). As a second marker for proliferation, we measured Ki-67 levels in splenic B cells of mb1-Cre;Pten^{fl/+};Eμ-TCL1 and mb1-Cre;Eμ-TCL1 control mice by flow cytometric analysis. Again, no significant difference in Ki-67 expression levels could be observed (Figure 6E, right; *Online Supplementary Figure S5F*). So, we assume that loss of PTEN expression does not promote CLL transformation towards RT.



Continued on following page.

Figure 6. A single deleted *Pten* allele is enough to accelerate the onset of chronic lymphocytic leukemia. (A) Flow cytometric analysis of B cells from the spleens of mb1-Cre;*Pten*^{fl/+};E μ -TCL1 mice. Dot plot of the anti-B220 vs. anti-CD5 staining after gating on CD19⁺ B cells. The gated regions in the dot plots correspond to chronic lymphocytic leukemia (CLL) cells (CD19⁺ B220^{low} CD5⁺) and healthy mature B cells (CD19⁺ B220⁺ CD5⁻). The numbers in the dot plots indicate the mean relative frequency of cells in the gate. (B) Quantification of the relative number of (CD19⁺ B220^{low} CD5⁺) splenic mouse B cells from mb1-Cre;*Pten*^{fl/+};E μ -TCL1 (blue filled bars) and mb1-Cre;E μ -TCL1 (red filled bars) mice. Graphs are presented as mean \pm standard error of the mean (SEM). Four asterisks (****) indicate $P < 0.0001$, P -values were obtained using two-tailed Student's t -test. Results from 5 mice per group are shown. (C) Dot plot of the anti-IgM vs. anti-IgD staining after gating on CD19⁺ B220^{low} CD5⁺ (left) and CD19⁺ B220⁺ CD5⁻ (right). The gated regions in the dot-plots correspond to CLL cells (IgM^{high}IgD⁻) and healthy mature B cells (IgM⁺IgD^{high}). The numbers in the dot-plots indicate the mean relative frequency of cells in the quadrants. (D) Flow cytometric analysis showing histograms overlays of AKT-phosphorylation (left) and size (right) of splenic B cells from mb1-Cre;E μ -TCL1 (red line) and mb1-Cre;*Pten*^{fl/+};E μ -TCL1 mice (blue line). (E) Quantification of AKT phosphorylation (left) and Ki-67 (right) mean fluorescence intensity (MFI) in splenic mouse CLL B cells from mb1-Cre;*Pten*^{fl/+};E μ -TCL1 (blue filled bars) and mb1-Cre;E μ -TCL1 (red filled bars) mice. Graphs are presented as mean \pm SEM. Four asterisks (****) indicate $P < 0.0001$, P -values were obtained using two-tailed Student's t -test (**** $P < 0.0001$; ns=not significant). Results from 5 mice per group are shown. (F) Quantification of PHH3 positive cells of the splenic sections from diseased mb1-Cre;*Pten*^{fl/+};E μ -TCL1 and mb1-CreER^{T2}; E μ -TCL1 mice. Graphs are presented as mean \pm SEM; bars show the mean value of 6 analyzed pictures per spleen. P -values were obtained using two-tailed Student's t -test (ns=not significant). Results from 4 mice per group are shown.

PTEN is downregulated in human chronic lymphocytic leukemia cells

In order to test whether PTEN plays a role in the survival of human CLL, we analyzed its protein expression in B cells from human CLL blood samples. The patient-derived CLL samples were classified according to the presence (mutated, M-CLL) or absence (unmutated, U-CLL) of the mutation in the immunoglobulin heavy chain variable region gene (IGHV). An unmutated IGHV gene is a molecular marker in human CLL associated with poorer prognosis and shorter survival of the patients. As a control we used blood samples from HD (age 60+ years). Overall, we analyzed 14 M-CLL and 21 U-CLL samples as well as 16 HD samples for their PTEN protein expression in B cells using flow cytometry. Statistical analysis revealed a significantly decreased PTEN protein expression in CLL cells when compared to B cells from HD B1 and B2 (Figure 7B and E). In nine of 14 M-CLL (64.3 %) and 17 of 21 U-CLL samples (81 %) there was lower PTEN expression in CLL cells when compared to the mean of the HD B1 control cells (Figure 7B, E and F). The remaining CLL samples showed either similar or slightly higher PTEN protein levels relative to the mean of the HD samples (Figure 7F). As a control, the same samples showed no difference in size or when stained with the secondary Ab alone (Figure 7C). In order to assess whether the downregulation of PTEN protein expression in the 64.3 % M-CLL and 81 % U-CLL samples was controlled in a post-transcriptional or post-translational manner, we measured the PTEN mRNA transcript levels by RT-qPCR. The results revealed that the PTEN mRNA levels were significantly increased in 71.5 % of the M-CLL and in 73.3 % of the U-CLL samples when compared to the HD controls (Figure 7E and F). Therefore, we assumed that the PTEN protein levels in approximately two thirds of the analyzed CLL patients are likely downregulated by either translational repression via microRNA (miRNA) or in a post-translational manner. Indeed, the

repression of *PTEN* transcripts by miRNA has been already reported in many diseases.^{33,34}

Downregulation of PTEN expression by miRNA-21, miRNA-29 and PAX5

Among others, the miRNA miR-21 is known to target the tumor suppressor PTEN as the knockdown of miR-21 in a DLBCL cell line resulted in increased PTEN protein expression but did not affect the level of *PTEN* mRNA.³⁵ In order to address the miR-21 expression in human CLL, we performed miRNA isolation both from HD, M-CLL and U-CLL patients. The analysis by RT-qPCR revealed a significant increase in the amount of miR-21 in M-CLL and U-CLL B cells compared to HD control B cells (Figure 8A). The miR-29 family of miRNA, consisting of three members miR-29a, miR-29b and miR-29c, is highly expressed in cells of the adaptive immune response and has also been shown to regulate PTEN expression leading to an increased PI3K activity.³⁶ The ablation of miR-29 specifically in B lymphocytes results in an increase in PTEN expression and a decrease of the PI3K activity in mature B cells. We analyzed the expression levels of miR-29a, miR-29b and miR-29c in the HD, M-CLL and U-CLL patients' samples and could observe a significantly increased expression level of all three miR-29 family members in B cells from both M-CLL and U-CLL patients if compared to the HD controls (Figure 8B). Consequently, the expression of miR-21 and the miR-29 family was shown to be upregulated in human CLL cells, possibly accounting for the reduced PTEN protein levels in these cells.

A recent study has reported that the expression of miR-29 is controlled by PAX5.³⁷ Hence, we analyzed the protein expression of PAX5 in B cells from M-CLL and U-CLL patients as well as HD controls by flow cytometry. Indeed, we could observe significantly higher PAX5 protein expression levels in B cells derived from CLL patients compared to HD (Figure 8C and D, left). As a control, the same samples did not show a difference in size or in the isotype

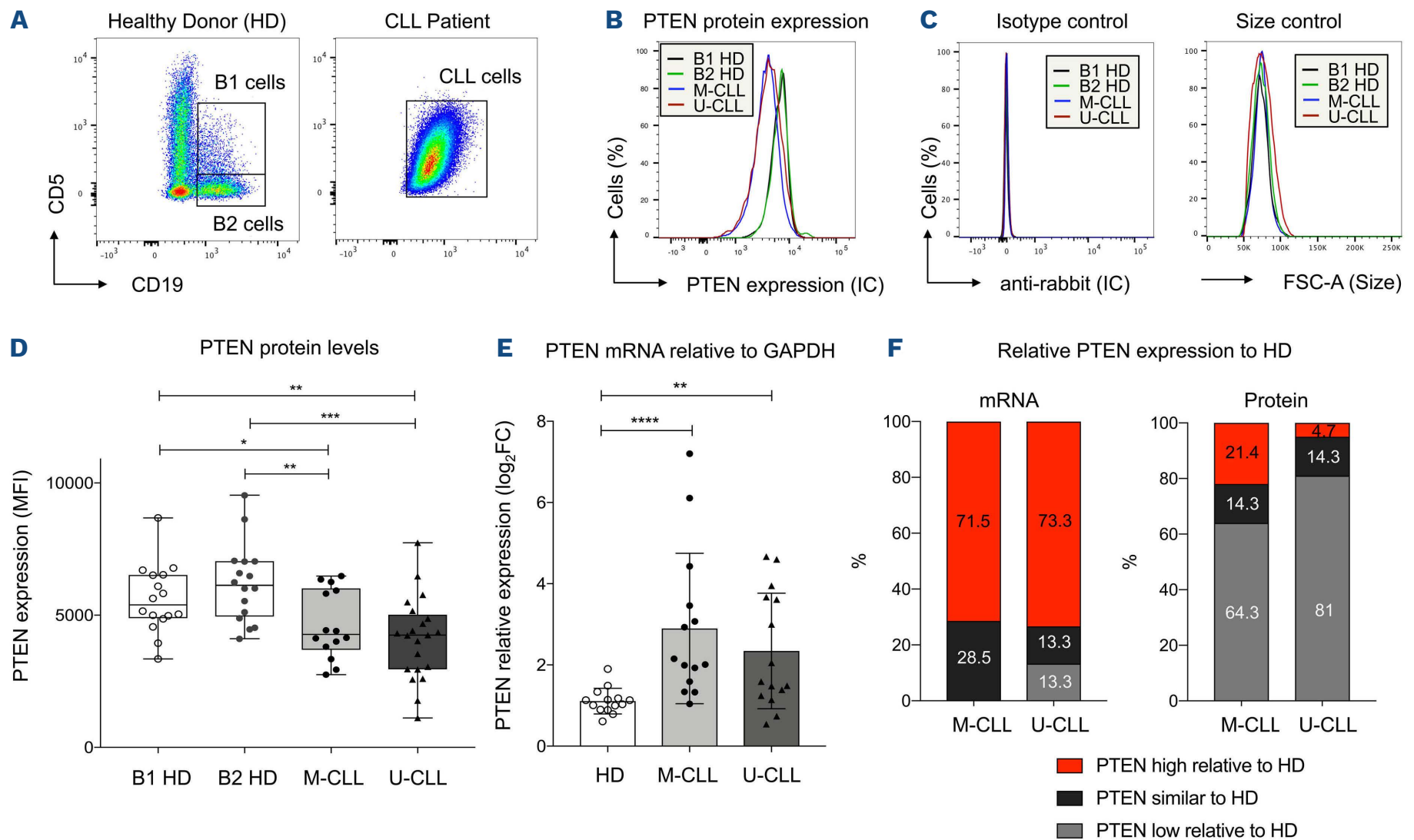


Figure 7. PTEN expression is downregulated in human chronic lymphocytic leukemia B cells. (A and B) Flow cytometric analysis of PTEN expression (B) in human blood samples from healthy donors (HD) B1 cells (black), B2 cells (green) and mutated chronic lymphocytic leukemia (M-CLL, blue) and unmutated CLL (U-CLL, red) patients. The histograms indicate the fluorescence intensity of PTEN protein expression of representative samples after gating on CD19⁺ and CD5⁺ cells from the U-/M-CLL patients and HD B1 cells (A). For the HD B2 cells, we gated on CD19⁺ and CD5⁻ cells (A, left). (C) Representative isotype control (C, left) and size control (C, right) of the flow cytometric analysis of PTEN expression in human blood samples from HD B1 cells (black), B2 cells (green) and M-CLL (blue) and U-CLL (red) patients. (D) Quantification of human blood samples from HD (age 60+) and CLL patients with and without a mutation in the IGHV gene (U-CLL and M-CLL). The plot indicates the mean fluorescence intensity (MFI) of PTEN protein expression after gating on CD19⁺ and CD5⁺ cells for the M-/U-CLL patients and the HD B1 cells. For the HD B2 cells we gated on CD19⁺ and CD5⁻ cells. The bars include median and standard deviation. *P*-values were obtained using two-tailed Student's *t*-test (**P*<0.05; ***P*<0.01; ****P*<0.001). Every dot or triangle represents an individual. (E) Real-time quantitative polymerase chain reaction (qRT-PCR) analysis of human blood samples from HD and U-/M-CLL. The plot indicates the levels of *PTEN* mRNA expression relative to the expression of the housekeeping gene GAPDH, including median and standard deviation. *P*-values were obtained using two-tailed Student's *t*-test (***P*<0.01; *****P*<0.0001). Every dot or triangle represents an individual. (F) Relative *PTEN* mRNA and protein expression in B cells from U-/M-CLL patients compared to the averaged expression of HD control. Red: samples show high *PTEN* mRNA/protein expression relative to HD, black: *PTEN* expression is similar relative to HD, grey: CLL patients have lower *PTEN*/mRNA levels relative to HD.

control staining (Figure 8D, right). Together, these data strengthen our hypothesis, that *PTEN* expression in CLL cells are post-transcriptionally repressed by high levels of the miRNA miR-21 and miR-29, the second upregulated by increased levels of PAX5 itself (Figure 8E).

Discussion

In this study we present a novel mouse model, which allows the Tamoxifen-inducible inactivation of Ig α (subsequently preventing BCR assembly and expression on the cell surface) in a mouse CLL model.

Our findings demonstrate that loss of mature B cells after the ablation of the BCR in combination with the anti-IL-7R treatment is an intrinsic feature of B cells and not due to their reduced production. Consistent with previous findings,^{25,38-40} we confirm here that mature peripheral B cells rely on their BCR for survival, as almost the complete B cell pool is lost within 2 months after Ig α inactivation. We took advantage of the mb1-CreER^{T2} mouse strain's efficient recombination of the Ig α locus and applied it to the E μ -TCL1 CLL mouse model, in which we could successfully ablate Ig α .

One major finding of this study is that in the E μ -TCL1 mouse model, the maintenance of CLL cells requires BCR

expression because in the absence of Ig α 100-fold fewer CLL cells are maintained compared to the Ig α -sufficient control. Based on our results, we suggest that in the absence of the BCR PI3K-signaling is reduced, as demonstrated by a decrease in AKT phosphorylation and lower levels of BCL-2 and MCL-1. In addition, the loss of BCR expression in CLL cells results in slightly downmodulated NF κ B activity what might additionally contribute to the decreased BCL-2 expression levels. BCL-2 is important for the development and survival of mature naive B cells,⁴¹

and its overexpression partially rescues BCR-deficient B cells.⁴² We further show that ablation of the BCR reduces tumor size and prolongs the overall survival of mice with fully developed CLL.

Srinivasan et al. have shown that BCR-dependent signaling via the PI3K provides the crucial “tonic signal”, which is indispensable for the maintenance of resting mature B cells.²⁵ Although other studies have attributed the micro-environment with a role in CLL development and progression,⁴³ our results demonstrate that, the BCR alone

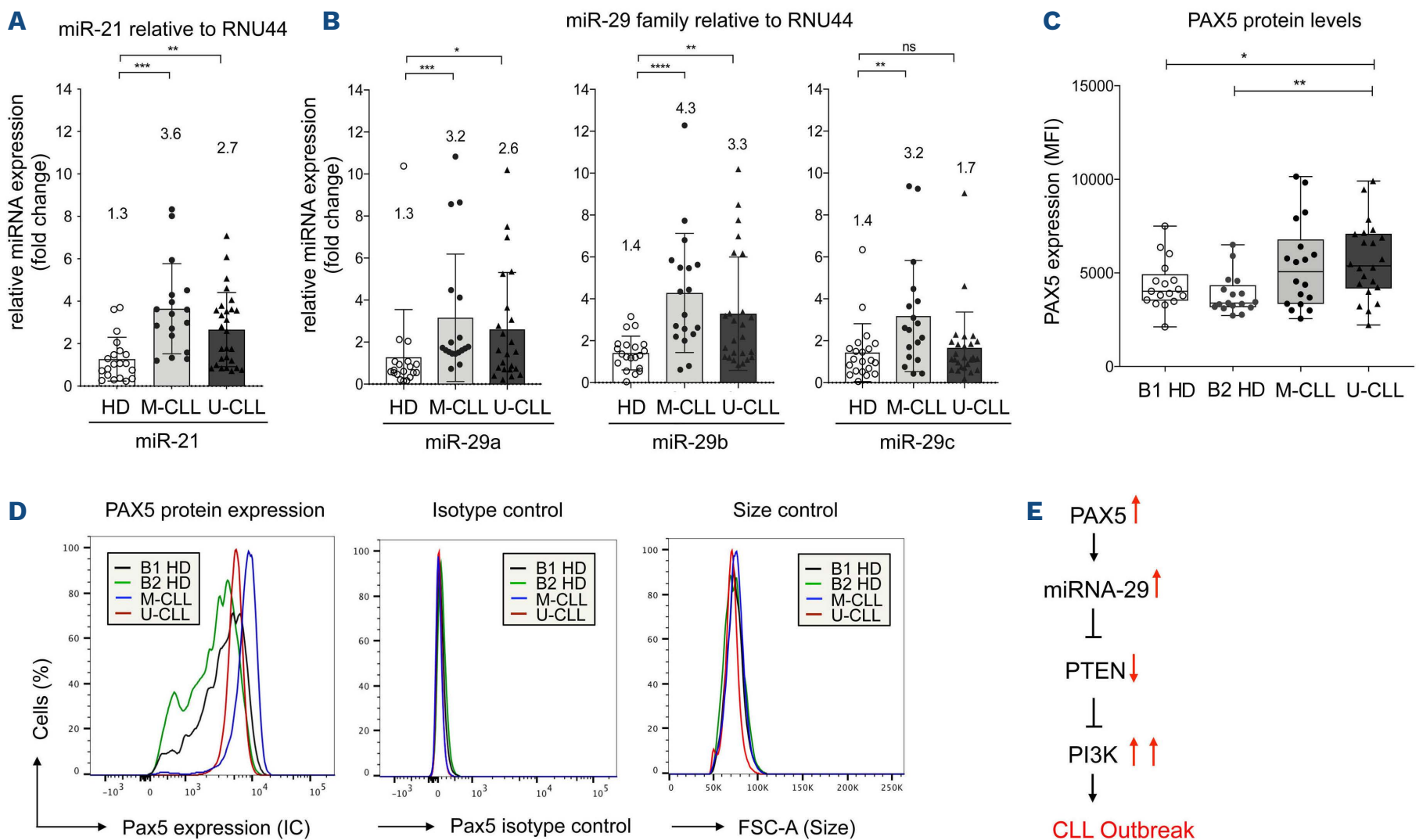


Figure 8. miR-21, miR-29 and PAX5 expression is increased in human chronic lymphocytic leukemia B cells. (A) Expression of miR-21 in chronic lymphocytic leukemia (CLL) patients (grouped: mutated and unmutated IgH V_H) and in the healthy donor (HD) control group (age: 60+ years) assessed by real-time quantitative polymerase chain reaction (qRT-PCR). The plot indicates the expression level of the microRNA (miRNA) miR-21 relative to the expression of the small-nucleolar RNA RNU44 used as endogenous control. Mean \pm standard error of the mean (SEM); numbers in the graph indicate the mean of each group. *P*-values were obtained using Mann-Whitney U-test (***P*<0.01; ****P*< 0.001). Every dot or triangle represents an individual. (B) Expression of the miR-29 family in CLL patients (grouped: mutated and unmutated IgH V_H) and in the HD control group (age: 60+ years) assessed by qRT-PCR. The plot indicates the expression levels of the miR-29 family members miR-29a, miR-29b, miR-29c relative to the expression of the small-nucleolar RNA RNU44 used as endogenous control. Mean \pm SEM; numbers in the graph indicate the mean of each group. *P*-values were obtained using Mann-Whitney U-test (**P*<0.05; ***P*<0.01; ****P*<0.001; *****P*<0.0001; ns=not significant). Every dot or triangle represents an individual. (C) Flow cytometric analysis of human blood samples gained from HD (age 60+ years) and CLL patients (grouped: mutated and unmutated IgH V_H). The plot indicates the mean fluorescence intensity (MFI) of PAX5 protein expression after gating on CD19⁺ and CD5⁺ cells for the mutated/unmutated CLL patients and the HD B1 cells. For the HD B2 cells we gated on CD19⁺ and CD5⁻ cells. Median \pm SEM. *P*-values were obtained using two-tailed Student's *t*-test (**P*<0.05; ***P*< 0.01; ****P*<0.001). Every dot or triangle represents an individual. (D) Flow cytometry analysis of PAX5 expression (left) in human blood samples of HD B1 cells (black), B2 cells (green) and CLL patients with mutated (blue) and unmutated (red) IgH V_H. The histograms indicate the fluorescence intensity of PAX5 protein expression of representative samples after gating on CD19⁺ and CD5⁺ cells for the CLL mutated/unmutated patients and the HD B1 cells. For the HD B2 cells we gated on CD19⁺ and CD5⁻ cells. Representative isotype control (middle) and size control (right) of the flow cytometric analysis are also shown. (E) Schematic representation of our working hypothesis. Upregulated PAX5 protein expression leads to higher expression of miR-29 family miRNA, which in turn inhibits the transcription of *PTEN* decreasing PTEN protein expression. This in turn increases the PI3K activity, which might lead to the development of CLL.

dictates the fate of the CLL cells in the E μ -TCL1 mouse model by activating the PI3K pathway, the key component of chronic active BCR signaling in mouse CLL.⁴⁴ This points out the importance of the BCR as a scaffold and platform for signaling emanating from different stimuli. Therefore, our results establish that BCR expression *per se* is required and indispensable to keep mouse CLL cells alive. To our knowledge, this study provides the first direct genetic evidence that the maintenance of mouse CLL cells depends on the BCR.

The second major finding of this study is that conditional deletion of the *Pten* gene and subsequent constitutively active PI3K signaling lead to an accelerated onset of CLL development in mice. CLL in E μ -TCL1 transgenic mice develops after long latencies.²⁰ This indicates that high expression of TCL1 is insufficient to drive transformation and that other genetic or epigenetic changes are presumably required. PTEN deficiency alone does not drive tumorigenesis in mature B cells;²⁶ however, based on our data, inactivation of PTEN with simultaneous overexpression of TCL1 accelerates the onset of CLL pathogenesis in young mice. We show that in PTEN-deficient TCL1-transgenic CLL cells AKT phosphorylation is increased compared to B cells only overexpressing TCL1. As PTEN-deficient splenic CLL cells are not susceptible to BCR stimulation with anti-IgM F(ab')₂ fragments, we believe that PTEN deficiency results in constitutive activation of the PI3K/AKT pathway. However, although Kohlhaas *et al.* recently reported that constitutive activation of AKT in a E μ -TCL1 mouse model results in RT³¹ we were unable to show this phenomenon in *Pten*^{fl/+};mb1-Cre;E μ -TCL1 mice with heterozygous *Pten* deletion. These results might be explained by differential progression and development of CLL in the respective mice. While we observe a significantly increased number of CLL cells in *Pten*^{fl/+};mb1-Cre;E μ -TCL1 mice compared to mb1-Cre;E μ -TCL1 control mice already at an age of 8 weeks (Figure 6A and B), this difference could not be detected in E μ -TCL1 mice with constitutive AKT activation before the mice reached an age of 7 months.

Spontaneous apoptosis of CLL cells *in vitro* has hampered the in-depth investigation of the mechanisms behind CLL maintenance. Cells from spleens of aged mb1-CreER^{T2};Pten^{fl/fl};E μ -TCL1 mice with high tumor load proliferated in culture without addition of growth factors. Flow cytometric analysis showed that the cells maintained the phenotype of the primary leukemia even after prolonged *in vitro* culture. To the best of our knowledge, E μ -TCL1 leukemia-derived cell lines have not been described to date. Recently, a similar phenomenon was observed by Chakraborty *et al.* wherein murine E μ -TCL1 leukemia cells exhibiting biallelic inactivation of *TP53*, *CDKN2A* and *CDKN2B* were also found to proliferate spontaneously *in vitro*.³⁹ Notably, cell lines from mb1-CreER^{T2};Pten^{fl/fl};E μ -

TCL1 were as susceptible to venetoclax as control cells from the mb1-CreER^{T2};E μ -TCL1 mice, showing that the loss of PTEN does not confer resistance to apoptosis. Moreover, the PTEN-deficient CLL-like culture cells still relied on BCR signals for proliferation as BCR signaling inhibitors caused decreased survival and proliferation of the cells *in vitro*. Interestingly, significantly increased cell death and decreased proliferation of PTEN-deficient mb1-CreER^{T2};Pten^{d/d};E μ -TCL1 culture cells in comparison to mb1-CreER^{T2};E μ -TCL1 leukemic cells could be observed due to NF κ B inhibitor treatment, indicating that the NF κ B pathway plays an important role in these PTEN-deficient CLL-like culture cells.

These PTEN-deficient CLL-like cell lines may be well suited for high-throughput screening of novel compounds for CLL treatment. Furthermore, the PTEN-deficient cells can be transplanted into immunodeficient mice and may be used in further *in vivo* studies. The rapid development of CLL in these mice may help to dissect signaling mechanisms of CLL cells within a reasonable time frame in contrast to the slow disease development in E μ -TCL1 mice. Therefore, this specifically provides a tool to develop novel treatment options for drug-resistant CLL.

It is remarkable that although splenic CLL cells from mb1-CreER^{T2};Pten^{fl/fl};E μ -TCL1 mice developed in culture after *ex vivo* deletion of *Pten*, they were not immortalized like the cells, in which *Pten* had been deleted *in vivo*. This may suggest that additional factors or additive mutations are required to promote transformation *in vivo*.

PTEN is tightly regulated by various non-genomic mechanisms including epigenetic silencing, post-transcriptional regulation by non-coding RNA, and post-translational modification.⁴⁵ Due to the high PTEN mRNA transcript levels in the analyzed human CLL samples which stand in contrast to the decreased PTEN protein expression, we assume that the PTEN downregulation in two thirds of overall 35 analyzed CLL samples might be regulated in a post-transcriptional manner mediated by non-coding RNA. miRNA comprise a large family of small non-coding RNA that emerged as post-transcriptional regulators of gene expression.⁴⁶ The microRNA miR-21, miR-155, miR-17-92 or miR-19 and miR-29, for instance, are post-transcriptional regulators of PTEN expression, which directly target PTEN and contribute to its reduced expression in CLL.⁴⁷ Moreover, several studies demonstrated that microRNA expression profiles can be used to distinguish normal B cells from malignant CLL cells and that miRNA signatures are associated with prognosis and progression of CLL.⁴⁸ Among other miRNA that have also been shown to regulate PTEN expression the miR-29 family is one of the critical miRNA that play a role in cancer pathogenesis.⁴⁹ It was revealed that E μ -miR-29 transgenic mice overexpressing miR-29 in B cells exhibit an expanded CD5+ B-cell population with 20% of the mice developed leukemia indicating

a role of miR-29 in the pathogenesis of B-CLL.⁵⁰ Our analysis of miR-29 expression in human CLL cells revealed that all three miR-29 family miRNA were significantly over-expressed in both M-CLL and U-CLL patient samples. Moreover, we could show that PAX5 expression is upregulated in human CLL patient samples, which might induce the upregulation of the miR-29 family miRNA. This stands in line with the recently published findings of Calderón *et al.* who identified PAX5 as an enhancer of PI3K signaling that downregulates PTEN expression in mature B cells, likely by controlling the abundance of *PTEN*-targeting miRNA.³⁷

In summary, our data illustrate that the loss of PTEN in murine CLL cells results in the accelerated development of the disease. This observation underscores the significance of PI3K signaling in the pathogenesis of CLL. In addition, the significant downregulation of PTEN expression in B cells of around two third of the analyzed CLL patients suggests an important role of PTEN in the development and maintenance of human CLL. It is conceivable that the decreased PTEN expression is induced by the increased levels of miR-21, miR-29 family and PAX5 expression in the analyzed human CLL cells as PAX5 is believed to restrain PTEN expression in B cells by controlling the expression of *PTEN*-targeting miRNA.³⁷ Conclusively, the work described in this paper strengthens the important role of PTEN as a tumor suppressor in CLL and raises a number of interesting questions that may help to design the potential use of *PTEN*-targeting miRNA inhibitor strategies for CLL.

Furthermore, we show that BCR loss fully abrogates the survival of CLL cells in mice. We therefore conclude that

PTEN expression sets a threshold for malignant transformation in the presence of BCR. Targeting the BCR itself, however, may be a major future achievement in combatting CLL, since antibodies against Ig β have been shown to be potent in depleting autoimmune and malignant B cells in mouse models and in preclinical studies.

Disclosure

No conflicts of interest to disclose.

Contributions

VS, AK, NA, and EH performed experiments and analyzed data. LN provided the Ig α TMF mice; KR provided ES cells targeted with Ig α TMF and discussed the study; EH and HJ designed the study and proposed the experiments; EH supervised the work and wrote the manuscript with VS. All the authors read the manuscript and discussed the results.

Acknowledgments

We thank Duygu Yağdıran, Karoline Lodd, Katharina Goehring, Lisa Göglér, Selina Fahrenholz, Stefanie Brey, and Andrea Schneider for their technical support and Ella Levit-Zerdoun for proof-reading the manuscript.

Funding

This work was supported by the DFG through SFB1074 (Experimental Models and Clinical Translation in Leukemia) projects A9, A10 and through TRR130 (B cells: Immunity and Autoimmunity) projects P01, P02, P04, P08 and C03, and through EXC294, and ERC advanced grants 694992 to HJ.

References

- Li Y, Wang Y, Wang Z, Yi D, Ma S. Racial differences in three major NHL subtypes: descriptive epidemiology. *Cancer Epidemiol.* 2015;39(1):8-13.
- Stevenson FK, Krysov S, Davies AJ, Steele AJ, Packham G. B-cell receptor signaling in chronic lymphocytic leukemia. *Blood.* 2011;118(16):4313-4320.
- Seda V, Mraz M. B-cell receptor signalling and its crosstalk with other pathways in normal and malignant cells. *Eur J Haematol.* 2015;94(3):193-205.
- Damle RN, Wasil T, Fais F, et al. Ig V gene mutation status and CD38 expression as novel prognostic indicators in chronic lymphocytic leukemia. *Blood.* 1999;94(6):1840-1847.
- Hamblin TJ, Davis Z, Gardiner A, Oscier DG, Stevenson FK. Unmutated Ig V(H) genes are associated with a more aggressive form of chronic lymphocytic leukemia. *Blood.* 1999;94(6):1848-1854.
- Stamatopoulos K, Agathangelidis A, Rosenquist R, Ghia P. Antigen receptor stereotypy in chronic lymphocytic leukemia. *Leukemia.* 2017;31(2):282-291.
- Philippen A, Diener S, Zenz T, Dohner H, Stilgenbauer S, Mertens D. SYK carries no activating point mutations in patients with chronic lymphocytic leukaemia (CLL). *Br J Haematol.* 2010;150(5):633-636.
- Dühren-von Minden M, Ubelhart R, Schneider D, et al. Chronic lymphocytic leukaemia is driven by antigen-independent cell-autonomous signalling. *Nature.* 2012;489(7415):309-312.
- Patel V, Balakrishnan K, Bibikova E, et al. Comparison of acalabrutinib, a selective Bruton tyrosine kinase inhibitor, with ibrutinib in chronic lymphocytic leukemia cells. *Clin Cancer Res.* 2017;23(14):3734-3743.
- Woyach JA, Bojnik E, Ruppert AS, et al. Bruton's tyrosine kinase (BTK) function is important to the development and expansion of chronic lymphocytic leukemia (CLL). *Blood.* 2014;123(8):1207-1213.
- Burger JA, Chiorazzi N. B cell receptor signaling in chronic lymphocytic leukemia. *Trends Immunol.* 2013;34(12):592-601.
- Ten Hacken E, Burger JA. Molecular pathways: targeting the microenvironment in chronic lymphocytic leukemia - focus on the B-cell receptor. *Clin Cancer Res.* 2014;20(3):548-556.
- Werner M, Hobeika E, Jumaa H. Role of PI3K in the generation and survival of B cells. *Immunol Rev.* 2010;237(1):55-71.
- Okkenhaug K, Vanhaesebroeck B. PI3K in lymphocyte development, differentiation and activation. *Nat Rev Immunol.* 2003;3(4):317-330.
- Downes CP, Ross S, Maccario H, Perera N, Davidson L, Leslie NR. Stimulation of PI 3-kinase signaling via inhibition of the tumor

- suppressor phosphatase, PTEN. *Adv Enzyme Regul.* 2007;47:184-194.
16. Thick J, Metcalfe JA, Mak YF, et al. Expression of either the TCL1 oncogene, or transcripts from its homologue MTCP1/c6.1B, in leukaemic and non-leukaemic T cells from ataxia telangiectasia patients. *Oncogene.* 1996;12(2):379-386.
 17. Herling M, Patel KA, Khalili J, et al. TCL1 shows a regulated expression pattern in chronic lymphocytic leukemia that correlates with molecular subtypes and proliferative state. *Leukemia.* 2006;20(2):280-285.
 18. Chen SS, Chiorazzi N. Murine genetically engineered and human xenograft models of chronic lymphocytic leukemia. *Semin Hematol.* 2014;51(3):188-205.
 19. Bresin A, D'Abundo L, Narducci MG, et al. TCL1 transgenic mouse model as a tool for the study of therapeutic targets and microenvironment in human B-cell chronic lymphocytic leukemia. *Cell Death Dis.* 2016;7(1):e2071.
 20. Bichi R, Shinton SA, Martin ES, et al. Human chronic lymphocytic leukemia modeled in mouse by targeted TCL1 expression. *Proc Natl Acad Sci U S A.* 2002;99(10):6955-6960.
 21. Kraus M, Alimzhanov MB, Rajewsky N, Rajewsky K. Survival of resting mature B lymphocytes depends on BCR signaling via the Igalpha/beta heterodimer. *Cell.* 2004;117(6):787-800.
 22. Hobeika E, Levit-Zerdoun E, Anastasopoulou V, et al. CD19 and BAFF-R can signal to promote B-cell survival in the absence of Syk. *EMBO J.* 2015;34(7):925-939.
 23. Suzuki A, Yamaguchi MT, Ohteki T, et al. T cell-specific loss of Pten leads to defects in central and peripheral tolerance. *Immunity.* 2001;14(5):523-534.
 24. Hobeika E, Thiemann S, Storch B, et al. Testing gene function early in the B cell lineage in mb1-cre mice. *Proc Natl Acad Sci U S A.* 2006;103(37):13789-13794.
 25. Srinivasan L, Sasaki Y, Calado DP, et al. PI3 kinase signals BCR-dependent mature B cell survival. *Cell.* 2009;139(3):573-586.
 26. Setz CS, Hug E, Khadour A, et al. PI3K-mediated Blimp-1 activation controls B Cell selection and homeostasis. *Cell Rep.* 2018;24(2):391-405.
 27. Liu J, Chen G, Feng L, et al. Loss of p53 and altered miR15-a/16-1short right arrowMCL-1 pathway in CLL: insights from TCL1-Tg;p53(-/-) mouse model and primary human leukemia cells. *Leukemia.* 2014;28(1):118-128.
 28. Lee HJ, Gallardo M, Ma H, et al. p53-independent ibrutinib responses in an Emu-TCL1 mouse model demonstrates efficacy in high-risk CLL. *Blood Cancer J.* 2016;6(6):e434.
 29. Landau DA, Tausch E, Taylor-Weiner AN, et al. Mutations driving CLL and their evolution in progression and relapse. *Nature.* 2015;526(7574):525-530.
 30. Alkhatib A, Werner M, Hug E, et al. FoxO1 induces Ikaros splicing to promote immunoglobulin gene recombination. *J Exp Med.* 2012;209(2):395-406.
 31. Kohlhaas V, Blakemore SJ, Al-Maari M, et al. Active Akt signaling triggers CLL toward Richter transformation via overactivation of Notch1. *Blood.* 2021;137(5):646-660.
 32. Kim JY, Jeong HS, Chung T, et al. The value of phosphohistone H3 as a proliferation marker for evaluating invasive breast cancers: a comparative study with Ki67. *Oncotarget.* 2017;8(39):65064-65076.
 33. Sandhu SK, Fassan M, Volinia S, et al. B-cell malignancies in microRNA Emu-miR-17~92 transgenic mice. *Proc Natl Acad Sci U S A.* 2013;110(45):18208-18213.
 34. Battistella M, Romero M, Castro-Vega LJ, et al. The high expression of the microRNA 17-92 cluster and its paralogs, and the downregulation of the target gene PTEN, is associated with primary cutaneous B-cell lymphoma progression. *J Invest Dermatol.* 2015;135(6):1659-1667.
 35. Bai H, Wei J, Deng C, Yang X, Wang C, Xu R. MicroRNA-21 regulates the sensitivity of diffuse large B-cell lymphoma cells to the CHOP chemotherapy regimen. *Int J Hematol.* 2013;97(2):223-231.
 36. Hines MJ, Coffre M, Mudianto T, et al. miR-29 sustains B cell survival and controls terminal differentiation via regulation of PI3K signaling. *Cell Rep.* 2020;33(9):108436.
 37. Calderon L, Schindler K, Malin SG, et al. Pax5 regulates B cell immunity by promoting PI3K signaling via PTEN down-regulation. *Sci Immunol.* 2021;6(61):eabg5003.
 38. Levit-Zerdoun E, Becker M, Pohlmeier R, et al. Survival of Igalpha-deficient mature B cells requires BAFF-R function. *J Immunol.* 2016;196(5):2348-2360.
 39. Chakraborty S, Martines C, Porro F, et al. B-cell receptor signaling and genetic lesions in TP53 and CDKN2A/CDKN2B cooperate in Richter transformation. *Blood.* 2021;138(12):1053-1066.
 40. Iacovelli S, Hug E, Bennardo S, et al. Two types of BCR interactions are positively selected during leukemia development in the Eμ-TCL1 transgenic mouse model of CLL. *Blood.* 2015;125(10):1578-1588.
 41. Nakayama K, Nakayama K, Negishi I, et al. Disappearance of the lymphoid system in Bcl-2 homozygous mutant chimeric mice. *Science.* 1993;261(5128):1584-1588.
 42. Lam KP, Kuhn R, Rajewsky K. In vivo ablation of surface immunoglobulin on mature B cells by inducible gene targeting results in rapid cell death. *Cell.* 1997;90(6):1073-1083.
 43. Ten Hacken E, Burger JA. Microenvironment interactions and B-cell receptor signaling in chronic lymphocytic leukemia: implications for disease pathogenesis and treatment. *Biochim Biophys Acta.* 2016;1863(3):401-413.
 44. Brown JR. The PI3K pathway: clinical inhibition in chronic lymphocytic leukemia. *Semin Oncol.* 2016;43(2):260-264.
 45. Song MS, Salmena L, Pandolfi PP. The functions and regulation of the PTEN tumour suppressor. *Nat Rev Mol Cell Biol.* 2012;13(5):283-296.
 46. Bartel DP. MicroRNAs: target recognition and regulatory functions. *Cell.* 2009;136(2):215-233.
 47. Musilova K, Mraz M. MicroRNAs in B-cell lymphomas: how a complex biology gets more complex. *Leukemia.* 2015;29(5):1004-1017.
 48. Calin GA, Liu CG, Sevignani C, et al. MicroRNA profiling reveals distinct signatures in B cell chronic lymphocytic leukemias. *Proc Natl Acad Sci U S A.* 2004;101(32):11755-11760.
 49. Pekarsky Y, Croce CM. Is miR-29 an oncogene or tumor suppressor in CLL? *Oncotarget.* 2010;1(3):224-227.
 50. Santanam U, Zanesi N, Efanov A, et al. Chronic lymphocytic leukemia modeled in mouse by targeted miR-29 expression. *Proc Natl Acad Sci U S A.* 2010;107(27):12210-12215.